DE-41 (DME)

NUST COLLEGE OF ELECTRICAL & MECHANICAL ENGINEERING

Design, Analysis and Optimization of Bladeless Fan

A PROJECT REPORT

DE-41 (DME)

Submitted by

NS BILAL ABDULLAH

ASC HAMMAD MUSTAFA

PC HASNAIN BADAR

NS MAHTAB UL DIN

BACHELORS

IN

MECHANICAL ENGINEERING

YEAR 2023

PROJECT SUPERVISOR

DR TARIQ TALHA

YEAR 2023

DECLARATION

We hereby declare that no portion of the work referred to in this Project Thesis has been submitted in support of an application for another degree or qualification of this of any other university or other institute of learning. If any act of plagiarism found, we are fully responsible for every disciplinary action taken against us depending upon the seriousness of the proven offence, even the cancellation of our degree.

COPYRIGHT STATEMENT

Abstract

The conventional ceiling fan employs fan blades to facilitate air distribution in the surrounding area, thereby inducing a cooling effect within the room. However, this airflow generates unpleasant noise resulting from the interaction between the blades and the air. Furthermore, conventional fans pose potential hazards to individuals in close proximity. In contrast, bladeless fans serve as an excellent alternative in addressing these issues, as they lack visible blades. Moreover, they exhibit lower power consumption, leading to reduced electricity costs. These fans have recently emerged for domestic applications, prompting research aimed at designing a bladeless fan with optimal performance. Computational Fluid Dynamics (CFD) techniques are utilized to analyze and evaluate the designed fan, followed by the fabrication of a prototype model. Literature reviews pertaining to this subject confirm the advantageous aspects of bladeless fans compared to conventional counterparts. However, it is worth noting that certain design improvements can be implemented to enhance the fan's ability to provide sufficient airflow to a larger number of individuals while increasing its overall performance.

TABLE OF CONTENTS

Chapter 1

Introduction

Chapter 2

Literature Survey

Chapter 3

Designing

Chapter 4

Analysis of Bladeless Fan

Chapter 5

3D Modeling & Structural Analysis

Chapter 6

Fabrication

Chapter 7

1. Introduction

The Bladeless Fan was first presented before the world by James Dyson in October 2009. It was then called the Dyson Air Multiplier. Though the concept was first given by the Japanese company, Toshiba, in 1981, James Dyson improved upon the design and technology to give us the Dyson Air Multiplier.

Working Mechanism:

A conventional fan with blades functions by pulling in air and dividing it into individual slices, which are then propelled towards the user at high velocities, resulting in a turbulent and forceful airflow. In contrast, the air multiplier operates in a distinct manner. It draws in air through a small aperture located in the pedestal base of the fan. An integrated brushless motor forces the air through asymmetrically aligned blades, referred to as a mixed-flow impeller, which enhances both the pressure and volume of the airflow. Subsequently, the air is propelled upwards through a wing-shaped opening positioned at the base of the hoop. This action generates a high-velocity stream of air while simultaneously attracting and multiplying the surrounding air volume by up to 15 times. Consequently, this coordinated pushing and pulling movement of air engenders a gentle airflow that eliminates the disruptive buffeting sensation commonly experienced with bladed fans.

It should be noted that a bladeless fan does, in fact, contain a blade; however, it remains concealed within the fan's motor. The more precise term for such a fan is an "Air multiplier."

The most notable advantage of bladeless fans lies in their minimal noise emission. By harnessing the air-multiplier technology, these fans draw in a significant amount of air and magnify it substantially. Not only do they consume less power, but they also exhibit remarkable power capabilities, accompanied by the added benefits of portability and safety. These fans have been engineered to minimize turbulence within the airflow, allowing for streamlined paths and the generation of a potent and smooth jet of air.

2. Literature Survey

2.1. Critical Parameters:

The Bladeless fan was invented in 2009, but the aerodynamic performance of this fan has not been studied numerically or experimentally for different conditions at that time. Here the effect of five geometric parameters is investigated on the performance of a Bladeless fan with a 30 cm diameter.

The studied parameters are height of fan cross section, outlet angle of the flow relative to the fan axis, thickness of the airflow outlet slit, hydraulic diameter, and aspect ratio for circular and quadratic cross sections.

The unsteady conservation of mass and momentum equations is solved to simulate three-dimensional incompressible flow in the Bladeless fan. Validating 3-D numerical simulations, the experimental results of a round jet are compared with the numerical simulation results because of their similarity with the bladeless fan and because data for bladeless fan does not exist.

The turbulence in the Bladeless fan is simulated by the standard k–ε turbulence model. In order to design the cross section of a Bladeless fan, Eppler 473 airfoil is chosen. The Eppler 473 airfoil is selected because it is an appropriate airfoil for low Reynolds numbers and the high similarity of this airfoil profile to the original cross section. The volume flow rate is calculated at a distance up to 3 times of the nozzle diameter in front of the fan.

The first parameter is the height of the fan cross section. Fig below shows the different sizes of cross sections and their dimensions are in 1.5 cm, 2 cm, 3 cm and 4 cm height cross sections are used to observe the effect of related parameters. Airfoil length and thickness of exiting region are constant for all case studies to keep the height of the fan cross section as the only varying parameter.

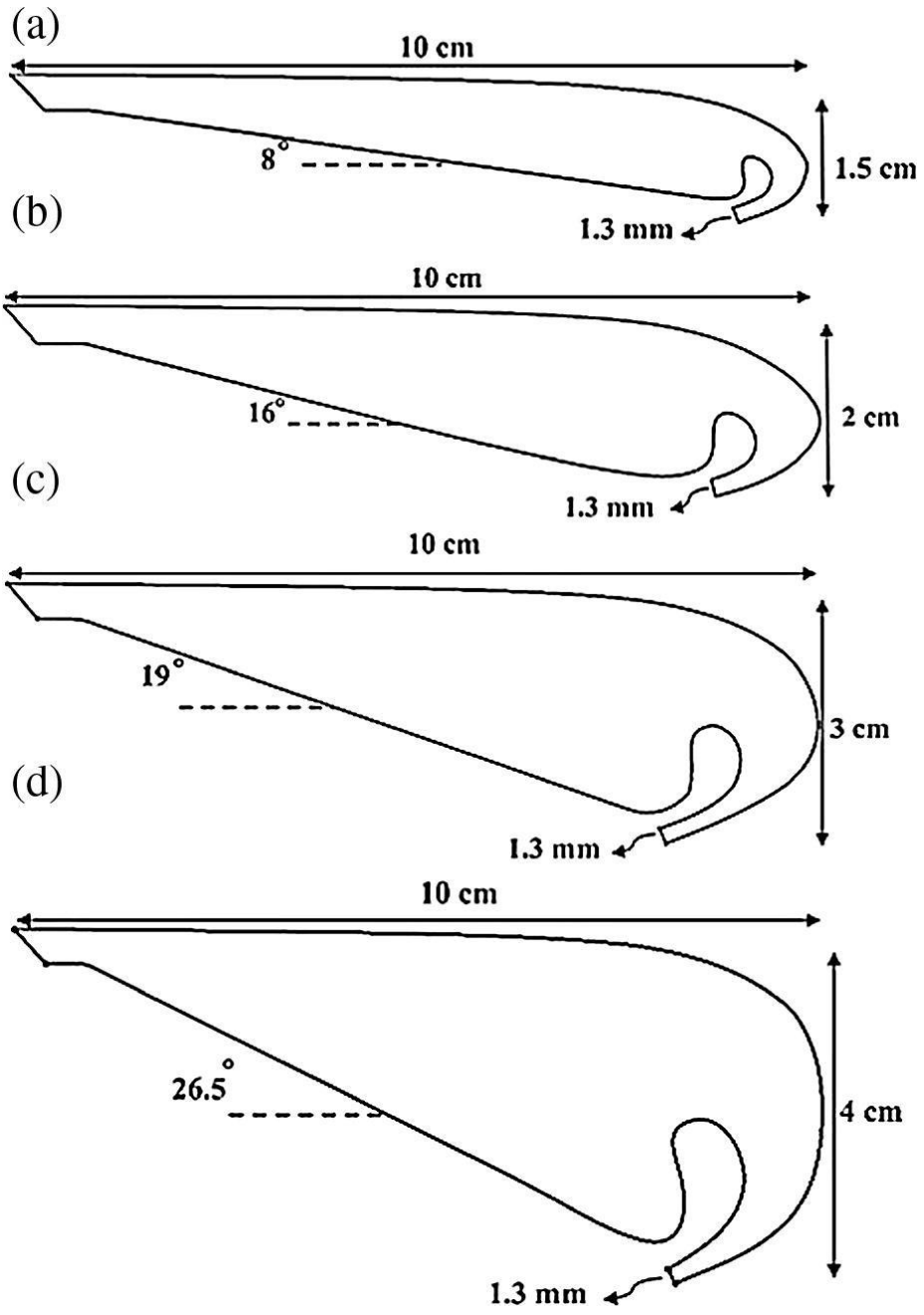

The second investigated parameter is the outlet angle of the flow relative to the fan axis. Outlet angles are assigned to be 10°, 13°, 16° and 20°. Also, the lengths of other airfoils are kept constant to keep the outlet angle the solo varying parameter. The thickness of the airflow outlet slit is 1 mm.

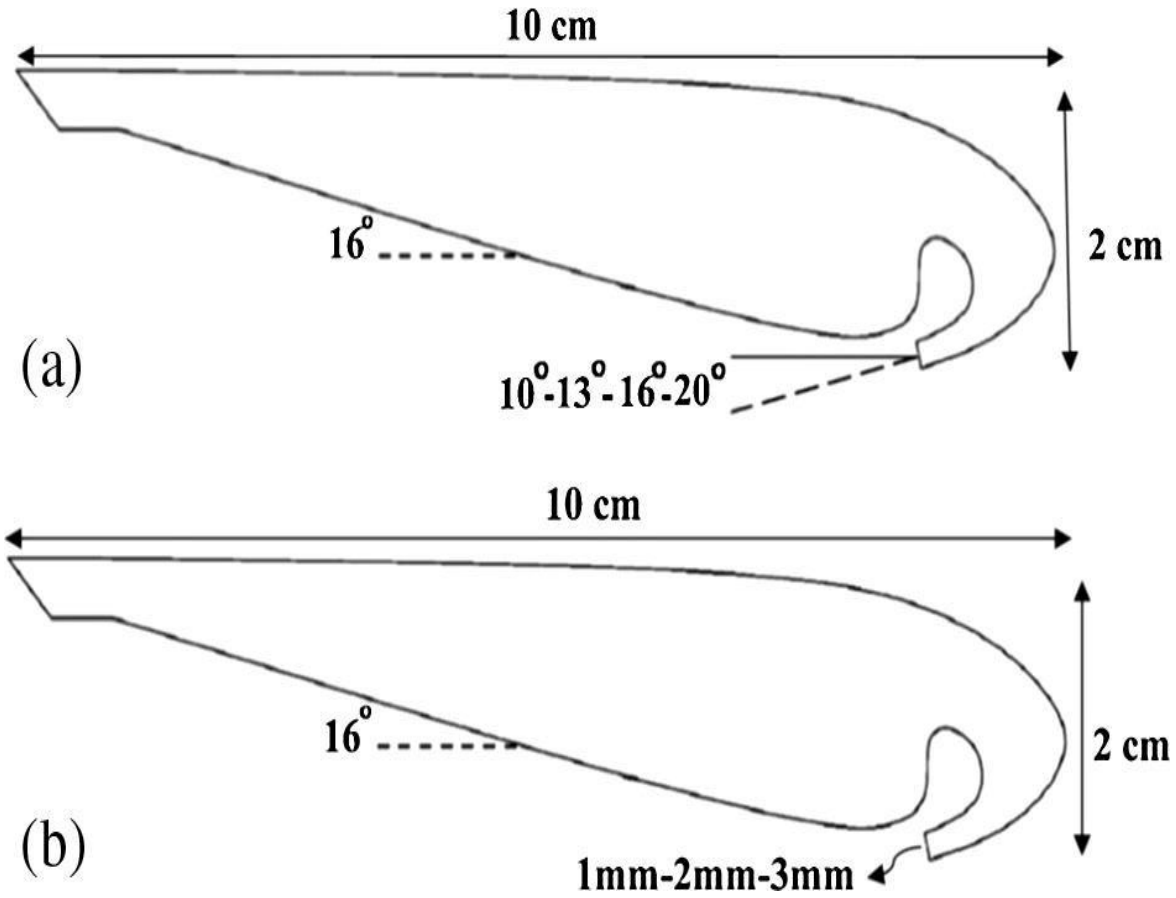

Thickness of the airflow outlet slit is the third studied parameter effecting on the Bladeless fan performance. Three outlet slits of 1 mm, 2 mm and 3 mm are considered with a constant airfoil length, height of cross section and outlet angle of flow (16°) are shown in above **fig b**.

Fourth parameter, three hydraulic diameters of 30 cm, 60 cm and 120 cm are considered for investigating the effect of hydraulic diameter size on Bladeless fan performance as shown in figure a below. The air outlet slit is a constant 4 mm for the mentioned case study.

Influence of aspect ratio for circular and square cross sections on the performance of a Bladeless fan is the last study parameter. Also, the effect of fan shape (circular or square) is studied Outlet slits for a circular and square fan are schematically shown in below figure b.

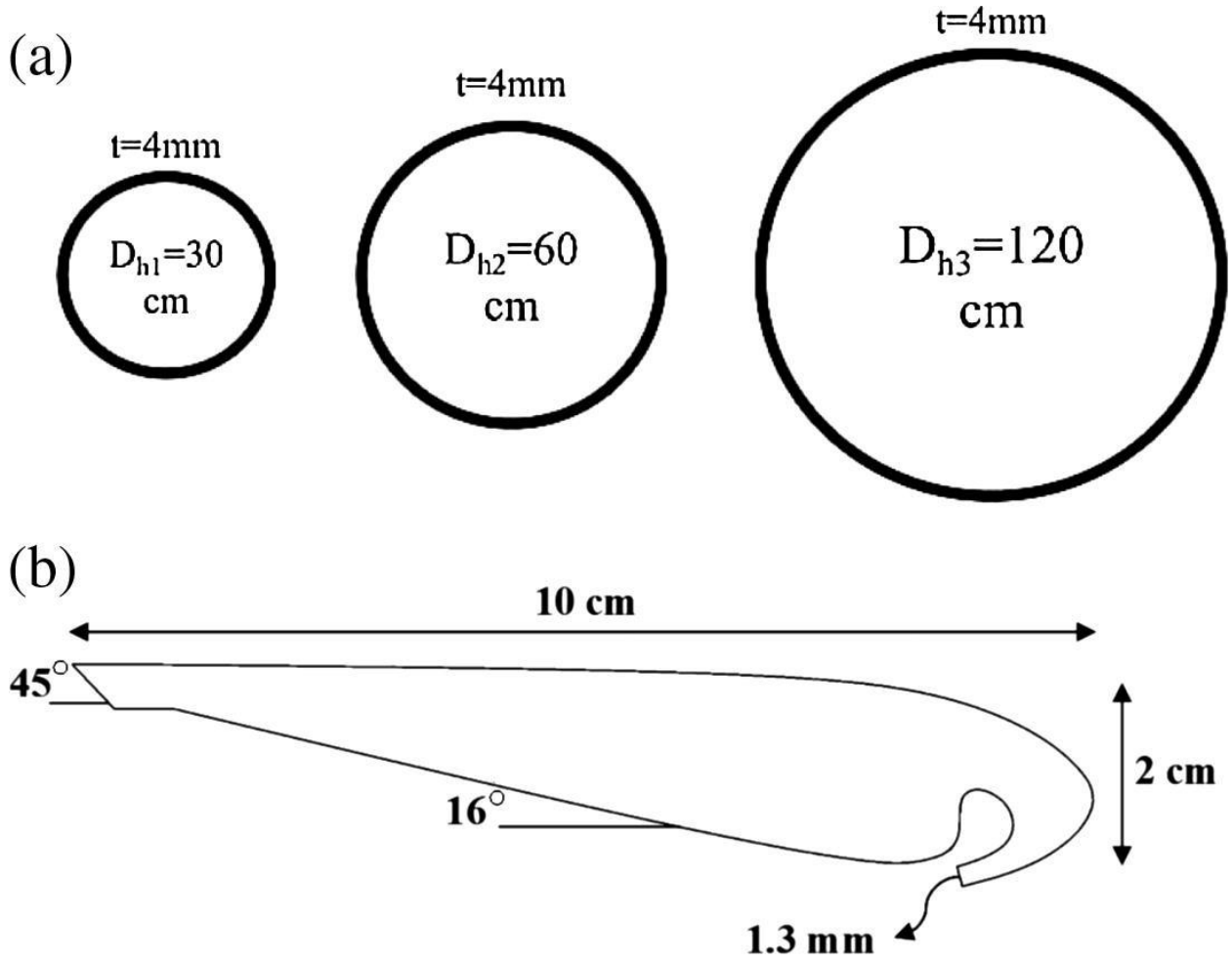
(a)
t=4mm
D_{h1}=30 cm
t=4mm
D_{h2}=60 cm
t=4mm
D_{h3}=120 cm
(b)
10 cm
45°
16°
2 cm
1.3 mm

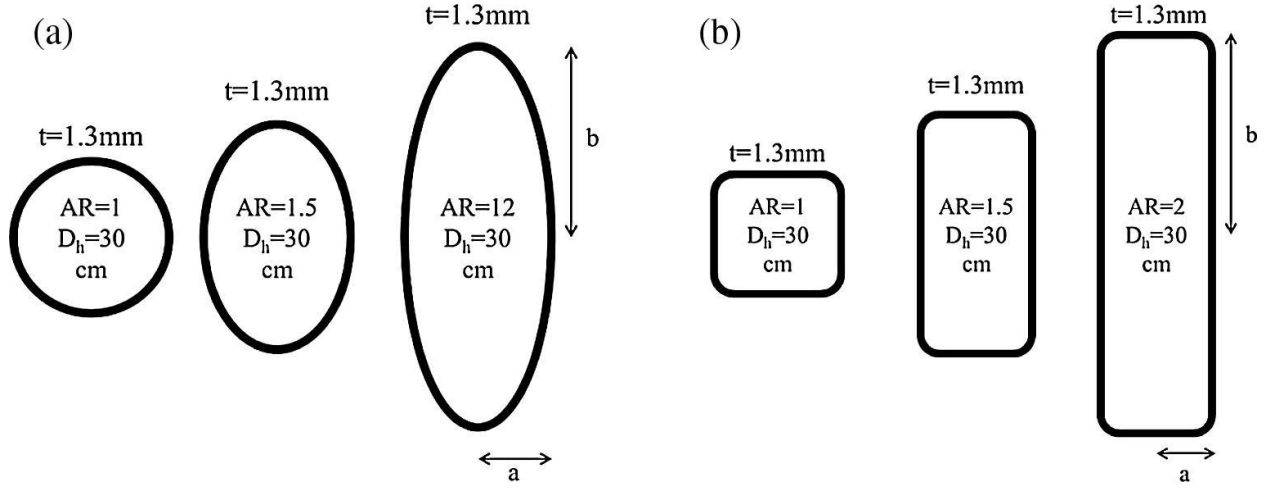
(a)
t=1.3mm
AR=1
D_h=30 cm
t=1.3mm
AR=1.5
D_h=30 cm
t=1.3mm
AR=12
D_h=30 cm
b
a
(b)
t=1.3mm
AR=1
D_h=30 cm
t=1.3mm
AR=1.5
D_h=30 cm
t=1.3mm
AR=2
D_h=30 cm
b
a

2.2.RESULTS:

i. Cross-sectional height of the fan:

Experimental data of a circular jet were used to validate the Bladeless fan simulation in this study. The k–ε standard turbulence model was used for. The first parameter is the cross-sectional height of the fan (CH). The flow rate increase curves in Fig a are shown for the fan section heights of 1.5, 2, 3 and 4 cm.

The multiplier factor *M* shows the ratio of the outlet flow rate to inlet flow rate from the fan. Fig a, b shows that the cross-sectional height of 3 cm has a higher *M* with respect to other thicknesses. As the amount of airfoil thickness decreases, due to a smaller Coanda effect, less airflow is drawn from behind the fan. However, when the cross-sectional height of fan increases, airflow sucked from behind will decrease because the area behind the fan decreases. So there is an optimal section thickness where the flow increase curve will have the maximum amount of Discharge ratio.

The results in Fig b show that the optimal value for the height of a 30 cm diameter Bladeless fan is 3 cm turbulence modeling. The inlet velocity was set to 60 m/s uniformly and the Reynolds number was 1.84.

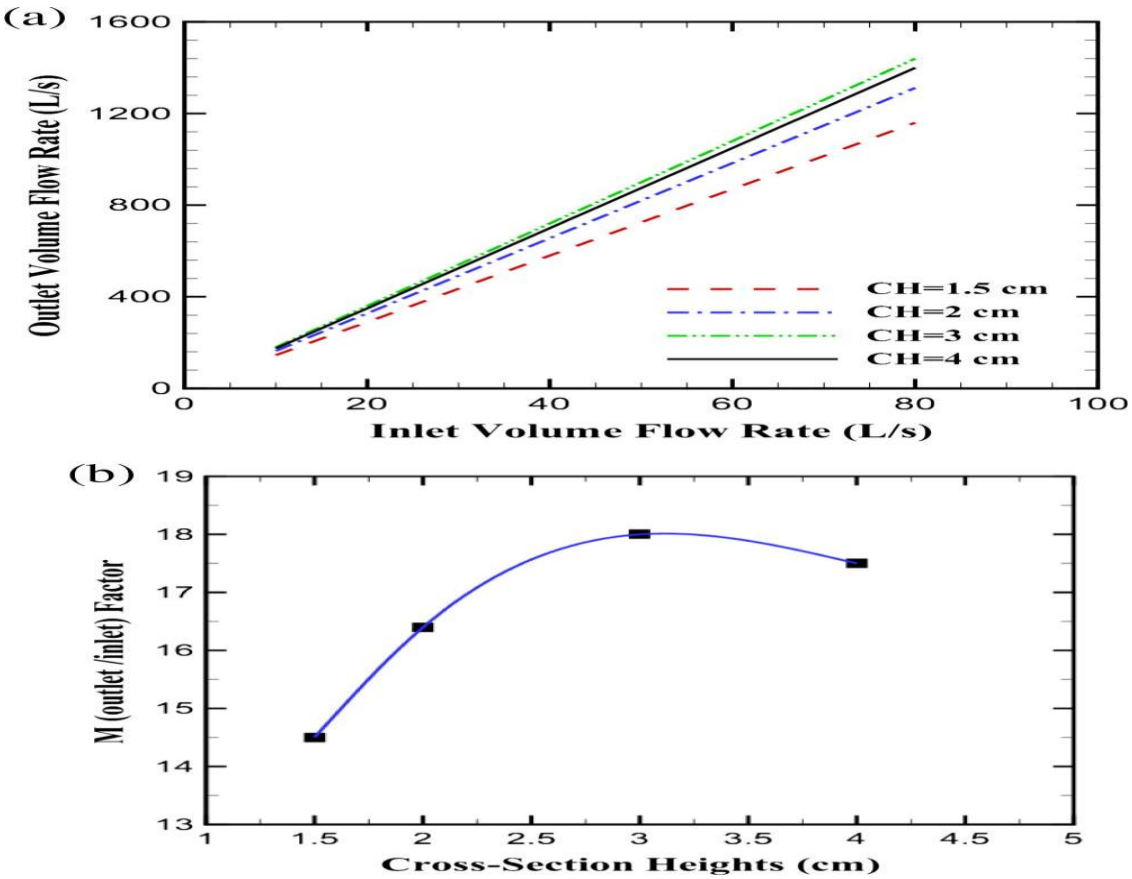

ii. Outlet Angle (OA):

The second geometrical parameter is the Outlet Angle (OA). The flow increase curves for angles of 10°, 13°, 16° and 20° are shown in the Fig below. This figure shows that when the exit flow angle is 16° the Discharge ratio is a little higher. Also, it shows that this parameter (outlet angle) does not have much effect on the flow increase curve.

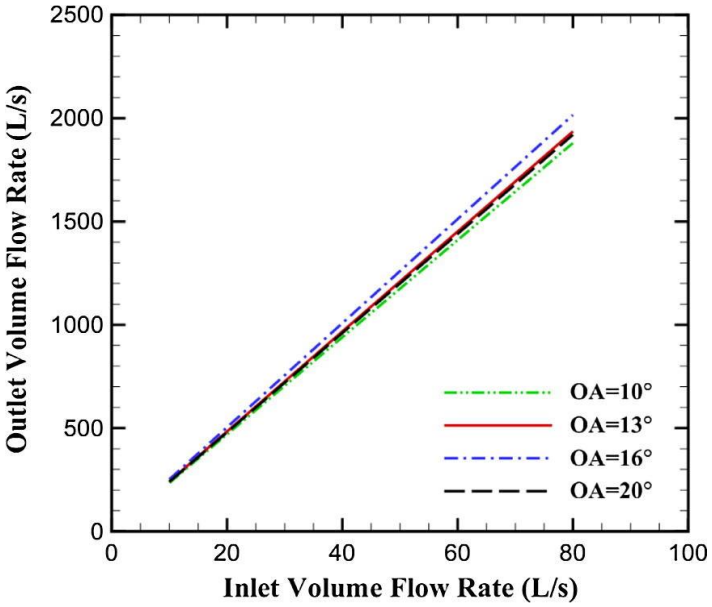

iii. Outlet thickness (OT):

The third parameter is the size of airflow outlet thickness (OT) from the fan. Flow increase curves for thicknesses of 1, 2 and 3 mm are shown in below Fig. This figure shows that by reducing the outlet thickness the multiplication factor increases.

The reason for this phenomenon is because of reducing the size of the outlet thickness. The outlet air velocity increases when outlet thickness decreases, so a large pressure gradient is created between in front and behind the fan.

Below Fig shows that the Discharge ratio is 25.2, 16.6 and 13.5, respectively, for outlet thicknesses of 1, 2 and 3 mm, respectively. The difference of obtained values for the Discharge ratio when outlet thicknesses change indicates that this parameter is one of the most influential geometric parameters on the increase or decrease of the Discharge ratio.

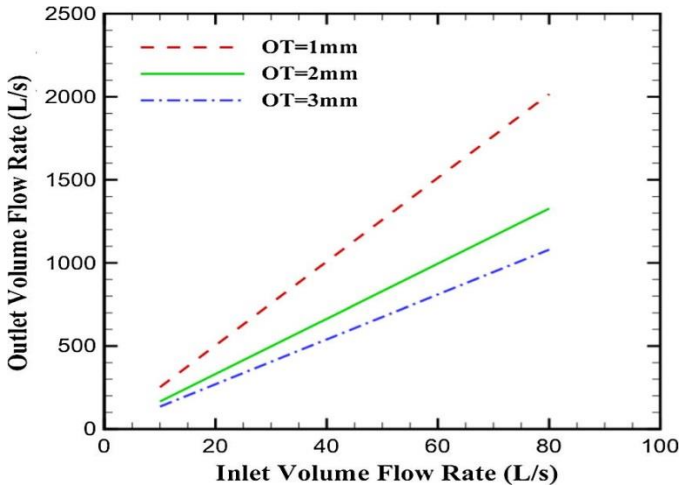

iv. Hydraulic diameter:

The fourth investigated parameter on the Bladeless fan is the hydraulic diameter. To evaluate the effect of this parameter, three fans with hydraulic diameters of 30, 60 and 120 cm are designed. In Fig below, the flow increase curves for different hydraulic diameters are shown. It is clear in this figure that for a constant input flow rate when the hydraulic diameter increases, the amount of outlet flow rate increases and the velocity magnitude of exhaust air from the fan is reduced.

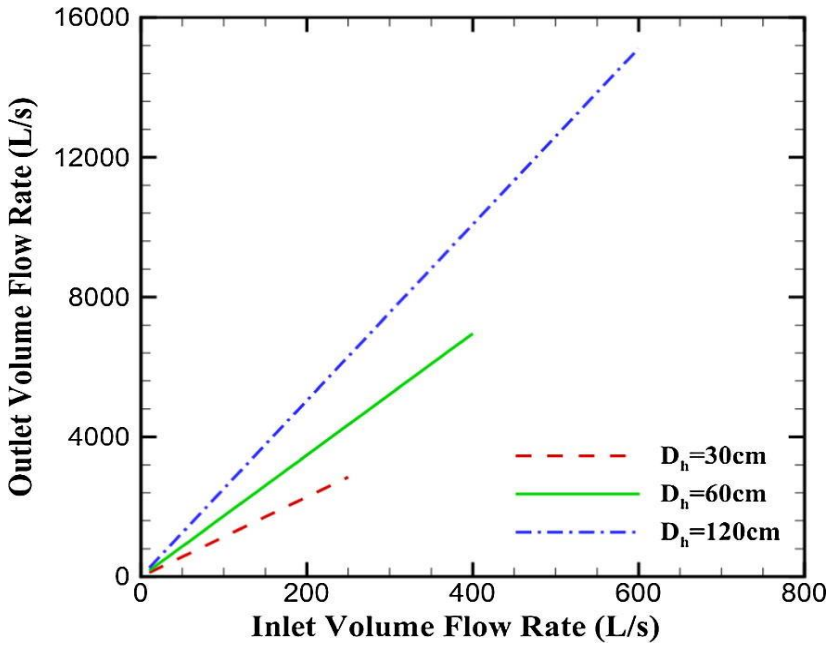

v. Aspect ratio:

The fifth geometric parameter is the effect of the aspect ratio of a Bladeless fan for square and circle shapes. The effect of aspect ratios of 1, 1.5 and 2 on the flow increase curve for a fan with a hydraulic diameter of 30 cm and an outlet thickness of 1.3 mm is shown in Figure. This figure shows that by increasing aspect ratio the Discharge ratio is reduced for a circular fan. In fact, the Discharge ratio will be higher when the aspect ratio is much closer to 1 (changing the elliptical shape into a circular shape).

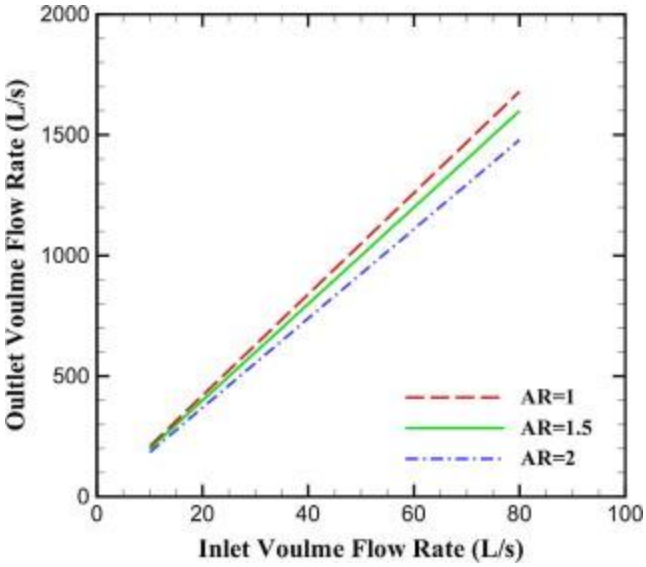

The effect of different aspect ratios on a square fan's flow increase curve is shown in below figure. This figure shows the Discharge ratio increases by decreasing the aspect ratio toward 1 (changing the rectangular shape into a square shape). This means that the aerodynamic performance of a Bladeless fan with a smaller aspect ratio is better.

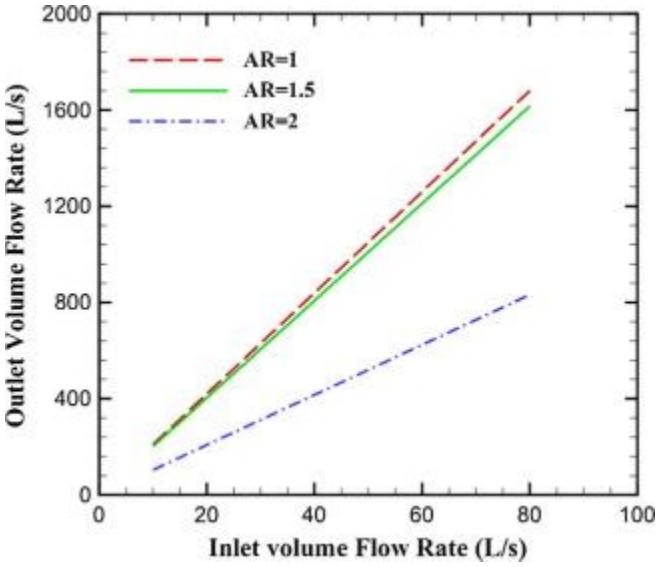

In below figure, the Discharge ratio is plotted for various aspect ratios to compare the results of a circle and square fan. Comparing the results shown in the figure indicates that the Discharge ratio for square and circle fans is almost equal when the aspect ratio decreases to 1. Also, the difference of the Discharge ratio between the two shapes increases significantly when the aspect ratio is about 2.

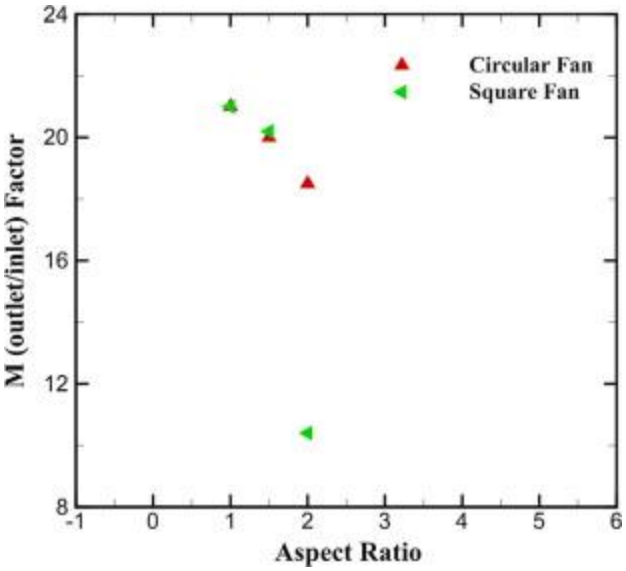

In figure below, for a better understanding of the airflow around the fan, the fan airflow path lines are shown. As indicated in this figure, airflow is drawn from behind and front sides of the fan and also shows that the exhausted airflow from a Bladeless fan is smooth and direct.

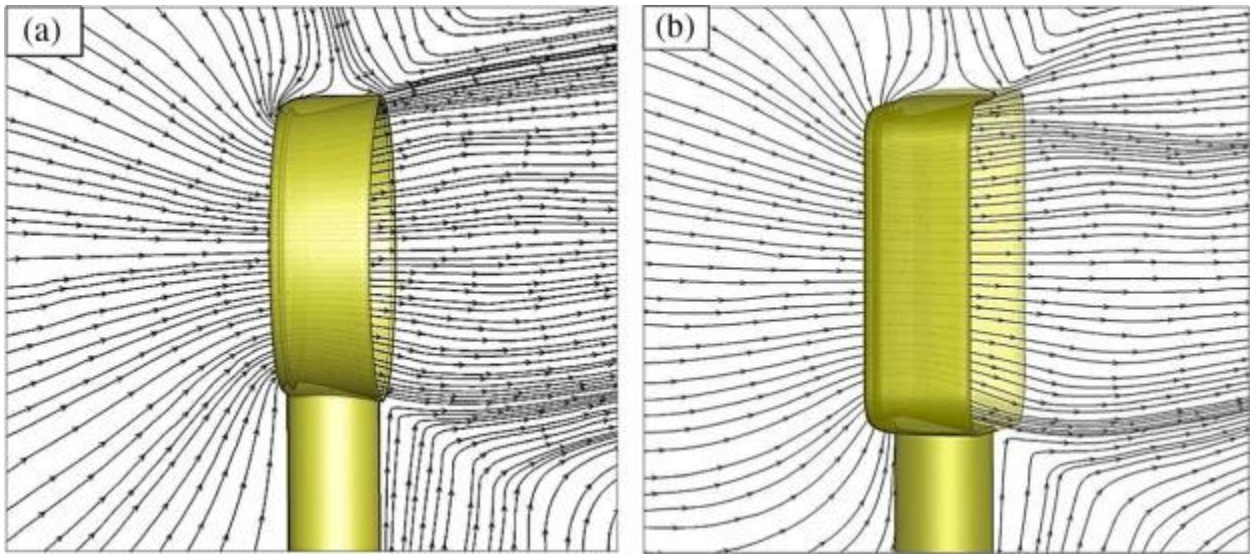

Path lines of airflow around two Bladeless fans, (a) circular, (b) square

2.3.Conclusions

Main outcomes of the study are as below:

- The obtained numerical results for cross sections with heights of 1.5, 2, 3 and 4 cm showed that the *Discharge ratio* has the maximum value for the height of 3 cm.
- For the outlet angles of 10°, 13°, 16° and 20°, the Discharge ratio for the outlet angle 16° was more than the others.
- The Discharge ratio increased significantly when the outlet thickness decreased.
- The Discharge ratio increased when the hydraulic diameter of fan increased.
- Whenever the aspect ratio is higher than 1, the Discharge ratio decreased considerably.
- The Discharge ratio of a square fan with high aspect ratios (about 2) is significantly less than the circle fan.

2.4. Clearly identified deliverables

- High Volume of Air Flow
- Steam line air flow
- Reduction in noise
- Volume flow rate control
- Fabrication

i. High Volume of Air Flow:

A bladeless fan is not entirely without blades. It simply means that the blades are hidden in the base. It has a mini motor with tiny blades. Despite the small sizes of the blades, it uses aerodynamics and physics-related properties to generate high airflow volume. Tiny exhaust vents intensify the pressure at which air passes and emits from the fan. The fluid dynamics principle of inducement amplifies the volume of generated airflow.

ii. Streamline air flow:

The blades of a conventional fan first chop the air before it reaches you, thus, causing buffeting. There is no issue of buffeting with a bladeless fan since it has no blades, so the flow of air is streamline.

iii. Reduction in Noise:

Traditional fans produce noise mainly due to movement of blades and turbulent flow of air while this noise level will be reduced in bladeless fan as their blades are located inside and flow of air produced from it is streamline

iv. Volume flow rate control:

The fan will have speed setting to control the volume flow rate of output air.

v. Fabrication:

After the analysis of design of our model, it will be fabricated. In fabrication outer ring and airfoil is manufactured using 3D printers.

2.5. Clearly identified SDG

Bladeless fans suck air inside them. Inside of the bladeless fan, entrainment of air takes place. Entrainment is straightforwardly an enriched way moving air. It creates negative air pressure within it. As the entrainment is produced inside it, it magnifies the air output up to 15 times as compared to conventional fan. Bladeless fans make use of Coanda effect. As the air continues to flow into the top ring, the air is pushed into a slit, that speed up the movement of air. So, they need and consumes less power than conventional fan. This mechanism makes them an energy-efficient device. Thus, less energy consumption results in lower electricity bills every month. It also produces less noise, thus reduced noise pollution. So, this project is in-line with the 7th SDG of the UN, that is to ensure affordable, reliable, sustainable and modern energy for all.

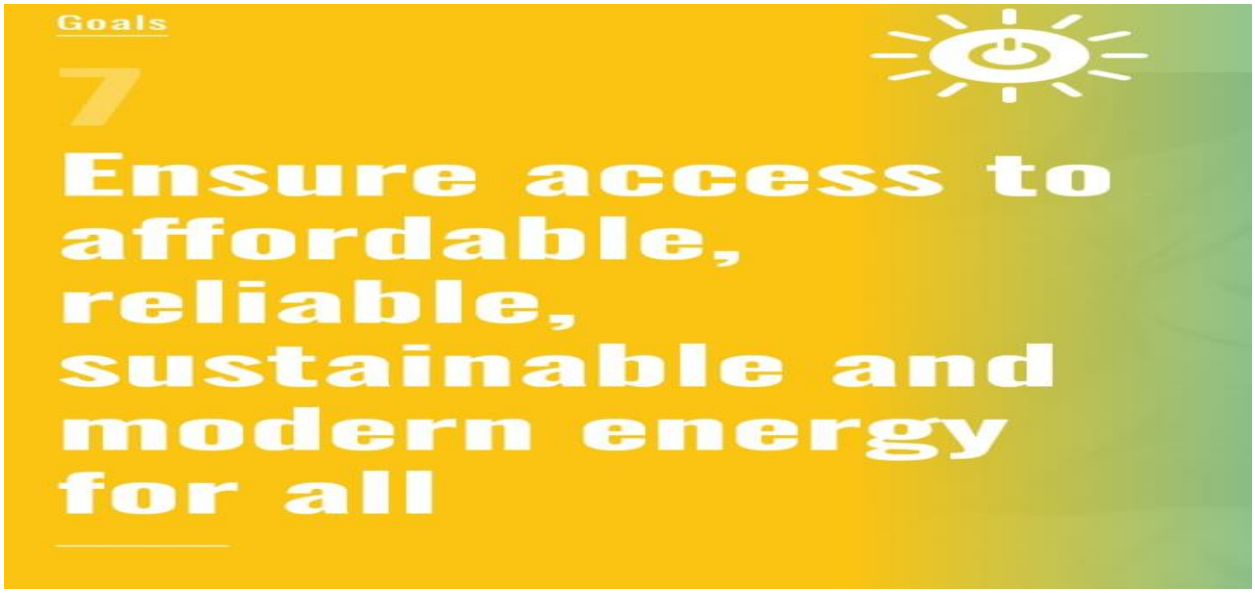

3. Designing

The design of a bladeless fan can vary depending on the specific model and the intended application, but the basic principles of the Coanda effect and the vortex created by the oscillating duct are always the same. The fan design also needs to be optimized for the

specific flow rate, pressure, noise level, and energy efficiency requirements of the application.

The design of a bladeless fan typically involves several key elements:

- Base Unit: This is the main body of the fan, which houses the motor and other components. It typically has a cylindrical shape and a smooth, sleek design.

- Circular ring: The circular ring in a bladeless fan typically refers to the air outlet, which is the part of the fan where the air is expelled. This ring is typically located at the top of the fan and is designed to maximize the flow of air.

- Motor: This is the power source that drives the fan. It typically uses a brushless DC motor which is more efficient and less noisy than traditional motors.

- Control Circuit: This is the part of the fan that controls the speed and other settings. It typically includes a microcontroller and other electronic components to manage the fan's performance.

- Air Inlet: This is the part of the fan where air is drawn in. It typically has a grill or other similar design to allow air to enter the fan.

- Air Outlet: This is the part of the fan where air is expelled. It typically has a smooth, circular design to maximize the flow of air.

3.1.Design of Airfoil:

Airfoil used is Eppler 473. Eppler 473 is a bladeless fan airfoil designed for use in wind tunnel testing and other aerodynamic applications. It is a highly efficient airfoil that uses a unique shape to generate lift and reduce drag, making it ideal for use in bladeless fan

systems. The airfoil features a thick, curved leading edge that smoothly transitions into a thin, tapered trailing edge, creating a streamlined shape that minimizes turbulence and maximizes airflow. The Eppler 473 is a versatile airfoil that can be used in a wide range of bladeless fan systems, and is especially well-suited for use in low-speed applications. With its smooth and efficient design, the Eppler 473 is an excellent choice for anyone looking to improve the performance of their bladeless fan system.

3.2.Reasons for choosing Eppler 473:

- Improved Aerodynamic Efficiency: The Eppler 473 airfoil has a unique design that allows for improved aerodynamic efficiency compared to other airfoils. This means that it can produce more airflow with less energy, making it an ideal choice for use in bladeless fans.

- Reduced Noise: The Eppler 473 airfoil is designed to reduce noise levels, making it a more comfortable option for use in spaces where noise levels are a concern.

- Increased Durability: The Eppler 473 airfoil is made from durable materials that can withstand the rigors of use in a bladeless fan. This means that it will last longer and require less maintenance than other airfoils.

- Improved Safety: The Eppler 473 airfoil eliminates the need for blades, which can be a safety hazard. This makes it a safer option for use in public spaces or in homes with children and pets.

- Enhanced Aesthetics: The Eppler 473 airfoil has a sleek, modern design that can enhance the aesthetic appeal of a bladeless fan. This makes it a great choice for use in spaces where design and aesthetics are important.

- Low Maintenance: The Eppler 473 airfoil does not require regular maintenance like other airfoils and blades, making it a more convenient option for use in bladeless fans.

3.3.Parameters of Eppler 473:

Airfoil is designed using MATLAB. Input parameters of airfoil can be changed in the MATLAB. MATLAB design of airfoil Eppler 473 is shown below.

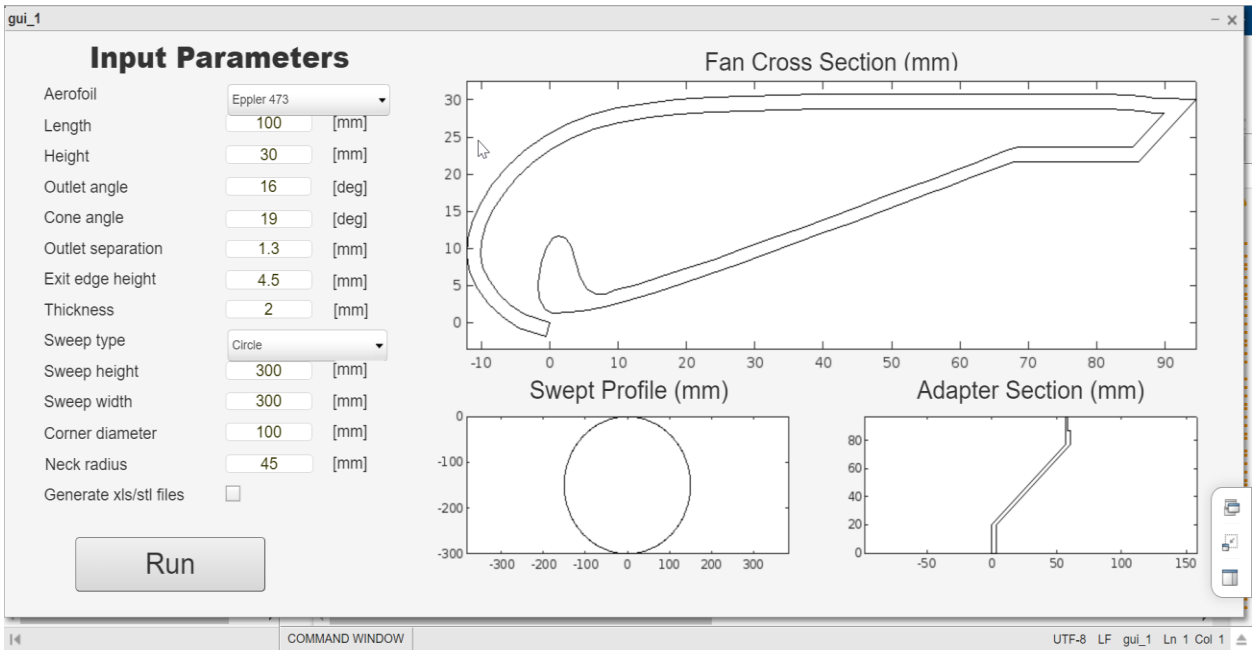

3.4. 3D Model of Bladeless Fan:

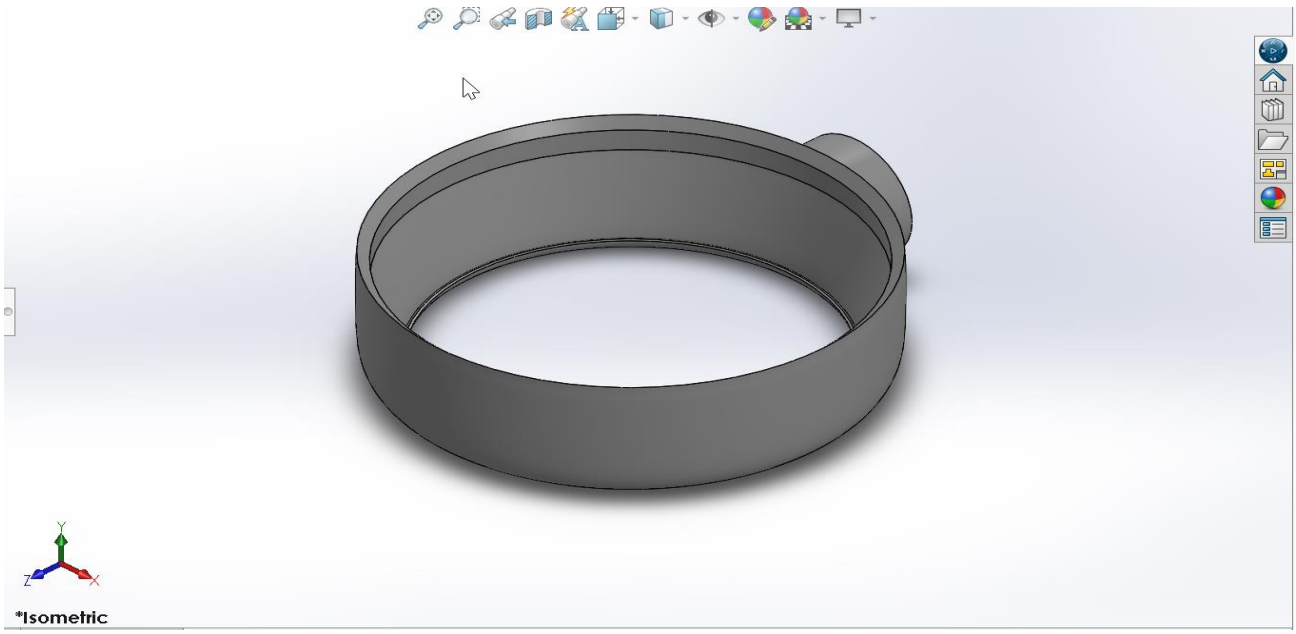

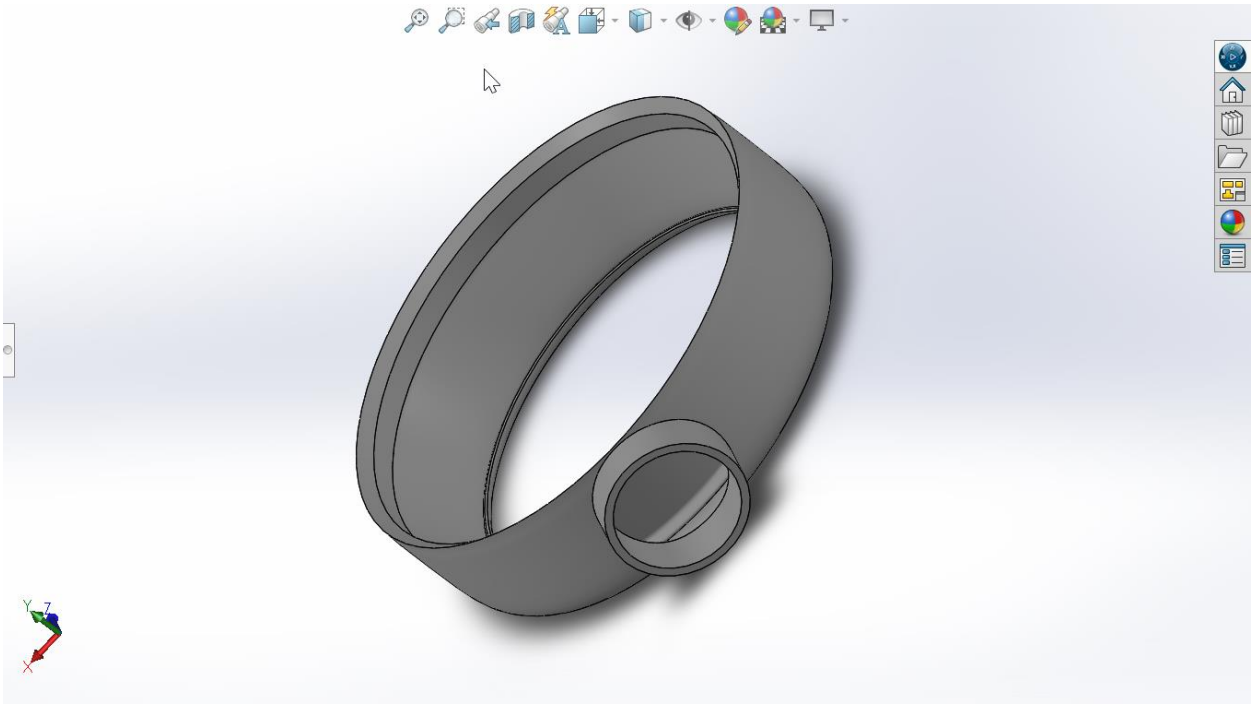

Isometric Views

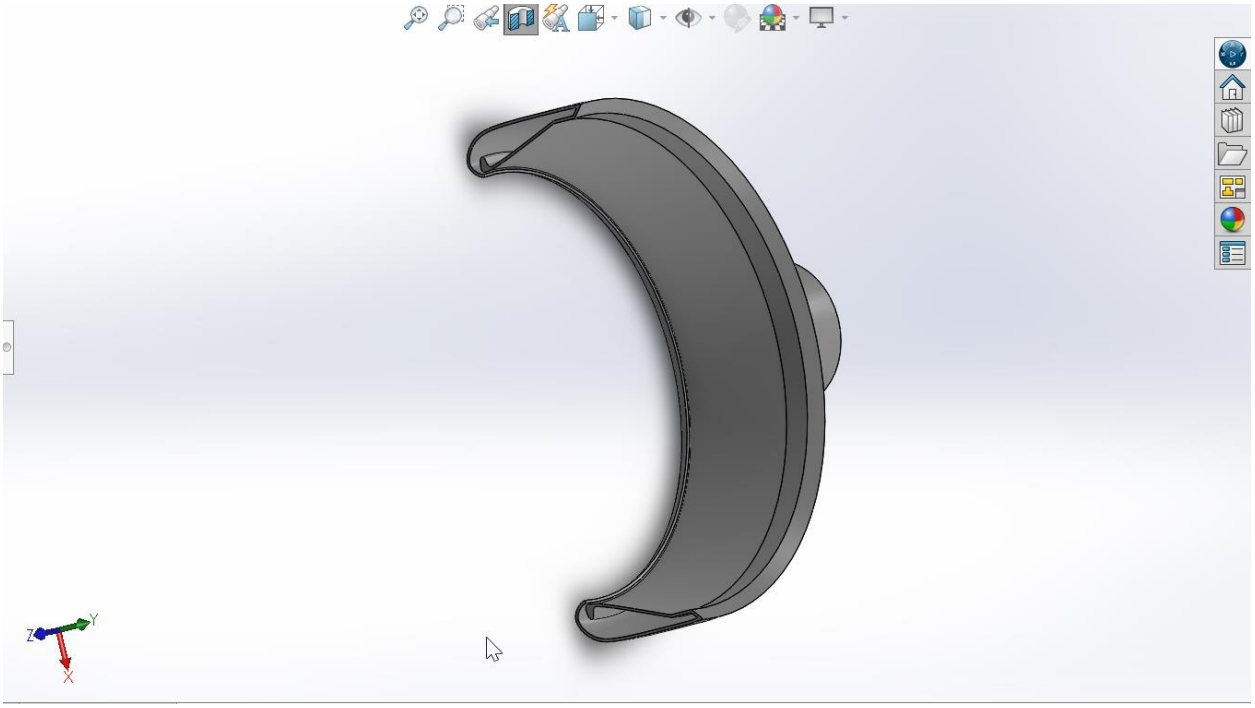

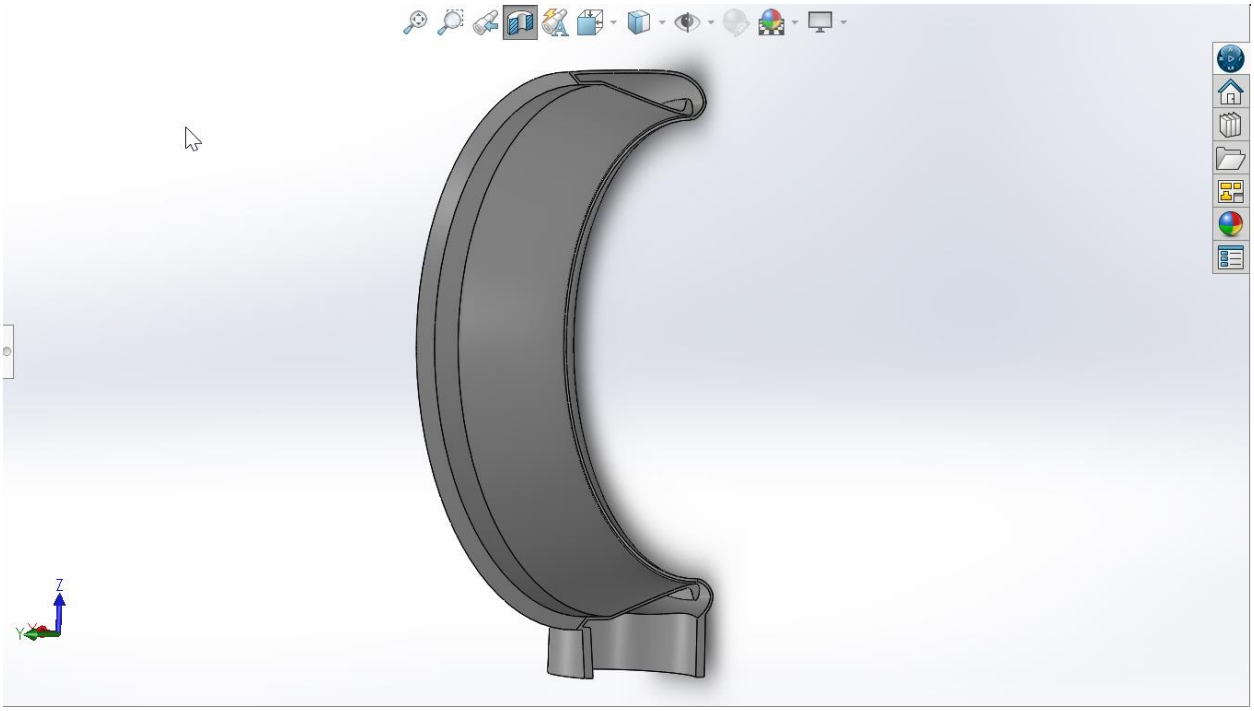

Section Views

4. Analysis of Bladeless Fan

4.1. Design of Fan:

The design of the bladeless fan involved specifying the dimensions and characteristics of the fan components. Using the MATLAB code, a simple bladeless fan was designed with specific parameters. The height of the airfoil was set to 25cm, determining the overall size of the fan. The slit thickness, which refers to the gap between the airfoil segments, was set to 1.3mm. This parameter controls the flow and turbulence of the air passing through the fan. Additionally, the outlet angle of the fan was set at 16°, determining the direction in which the air would be expelled.

Once the design was finalized using the MATLAB code, the 3D modeling of the fan was carried out using Autodesk Inventor software. This software allowed for the creation of a detailed three-dimensional representation of the fan based on the specified design parameters.

The modeling process involved accurately capturing the dimensions, shape, and features of the bladeless fan to ensure an accurate representation.

4.2.Domain Creation:

To create the domain for the bladeless fan, the 3D model designed in Autodesk Inventor was exported to software called SolidWorks. SolidWorks facilitated the creation of the fluid domain surrounding the fan. In this step, the fan part was subtracted from the surrounding fluid domain to generate a complete fluid domain that would encapsulate the fan.

The purpose of creating the fluid domain is to define the region where the flow analysis will take place. By subtracting the fan part from the fluid domain, the computational fluid dynamics (CFD) software can accurately simulate the airflow around and through the fan.

This process of domain creation ensures that the computational analysis focuses specifically on the region of interest, which in this case is the airflow behavior and performance of the bladeless fan. The resulting fluid domain provides the necessary environment for conducting further simulations and analysis to evaluate the fan's performance.

By combining the MATLAB code for initial fan design, the 3D modeling in Autodesk Inventor, and the domain creation in SolidWorks, a comprehensive design and modeling process is achieved. This process enables a detailed representation of the bladeless fan and sets the stage for subsequent analysis using computational fluid dynamics software to evaluate its performance and optimize its design if needed.

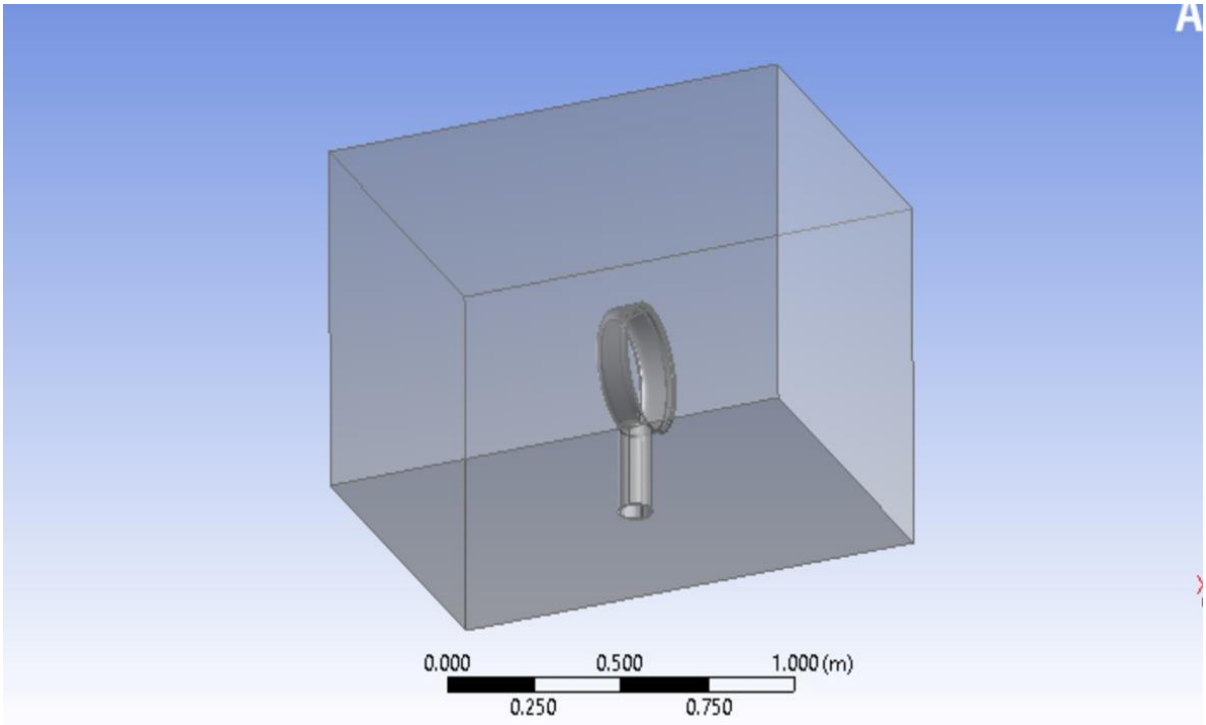

Domain

4.3.**Meshing**:

After the completion of the domain creation process in SolidWorks, the 3D model of the bladeless fan was exported to Ansys Software for further analysis. In Ansys, one crucial step is to mesh the domain, which involves dividing the fluid domain into a finite number of smaller elements. This meshing process is essential for accurate simulation and analysis of the fluid flow within the domain.

In this case, the meshing of the domain was performed with a grid size of approximately 5mm. The size of the mesh elements determines the level of detail and accuracy of the simulation results. Finer meshes capture smaller flow features but require more computational resources, while coarser meshes provide a quicker simulation but with potentially reduced accuracy. The chosen mesh size of 0.5mm provides a medium size meshing which strikes a balance between accuracy and computational efficiency.

To facilitate the analysis, the walls of the domain were assigned specific names or boundary conditions. This step allows for the application of appropriate boundary conditions to simulate real-world scenarios. In this case, the domain consisted of an inlet duct at the bottom of the fan and another inlet at the back wall of the domain, representing the airflow entering the system. The floor and the body of the fan were designated as no-slip boundaries, simulating the absence of relative motion between the fluid and the fan surface. This assumption is typically valid for solid surfaces. Lastly, the side walls of the domain were assigned as free boundaries, implying that no flow constraints or interactions were imposed on those surfaces.

By defining these boundary conditions, the simulation accurately represents the airflow behavior within the domain, taking into account the specific characteristics and design of the bladeless fan. The assigned boundary conditions ensure that the simulation accurately captures the flow dynamics, pressure distribution, and other relevant parameters.

Once the domain was meshed and the boundary conditions were set, the analysis using Ansys Software could be conducted. The simulation would provide valuable insights into the performance of the bladeless fan, including factors such as airflow patterns, velocity distribution, and pressure gradients. These results could be further analyzed and compared to design specifications or research objectives to evaluate the effectiveness and efficiency of the bladeless fan design.

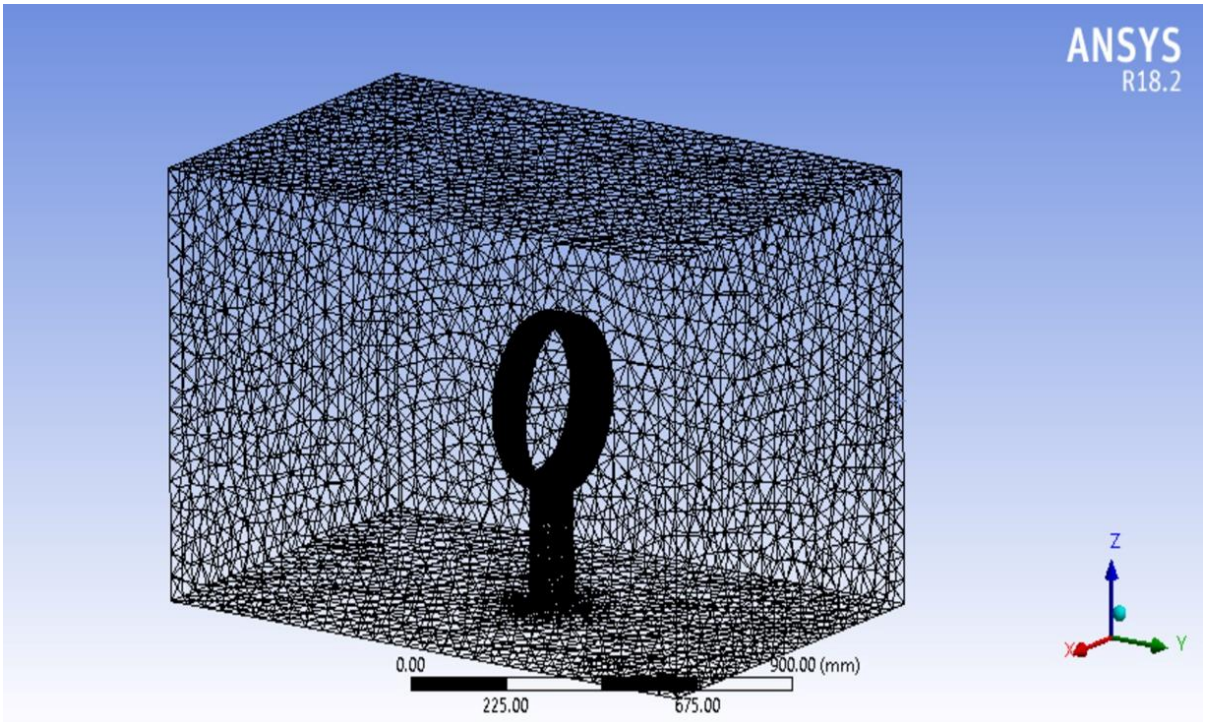

Meshed Part

4.4.Validation:

In the validation phase of the analysis, the results obtained from the simulation were compared with the findings of a previously conducted research study or reference data. This comparison serves to assess the accuracy and reliability of the simulation model and its ability to replicate real-world behavior.

In this case, the results of the simulation were compared to a research paper that had previously investigated a similar bladeless fan design or a comparable system. The specific metric used for comparison was the outlet flow rate, which indicates the amount of air flowing out of the fan.

Upon comparing the simulation results with the research paper, it was found that the outlet flow rate achieved in the simulation was approximately 85% in accordance with the values reported in the research paper. Specifically, the outlet flow rate in the simulation was

approximately 10 times higher than the inlet flow rate, while the research paper indicated a range of 12-15 times higher.

This comparison suggests that the simulation model performed reasonably well in replicating the flow behavior of the bladeless fan. The close agreement between the simulated results and the values reported in the research paper indicates that the simulation was able to capture the essential aspects of the fan's performance.

However, it is important to note that the slight discrepancy of 15% between the simulation and the research paper could be attributed to various factors, including differences in the specific fan design, boundary conditions, or assumptions made in the simulation. Further analysis and investigation may be needed to identify the exact reasons for this deviation and fine-tune the simulation model accordingly.

Nonetheless, the validation process provides confidence in the accuracy and reliability of the simulation results, demonstrating that the simulation captures the essential flow characteristics of the bladeless fan and can be utilized for further analysis and optimization.

Overall, the validation phase serves as an important step in assessing the credibility of the simulation model and ensuring that it can be relied upon for subsequent analysis, design improvements, and decision-making processes related to the bladeless fan system.

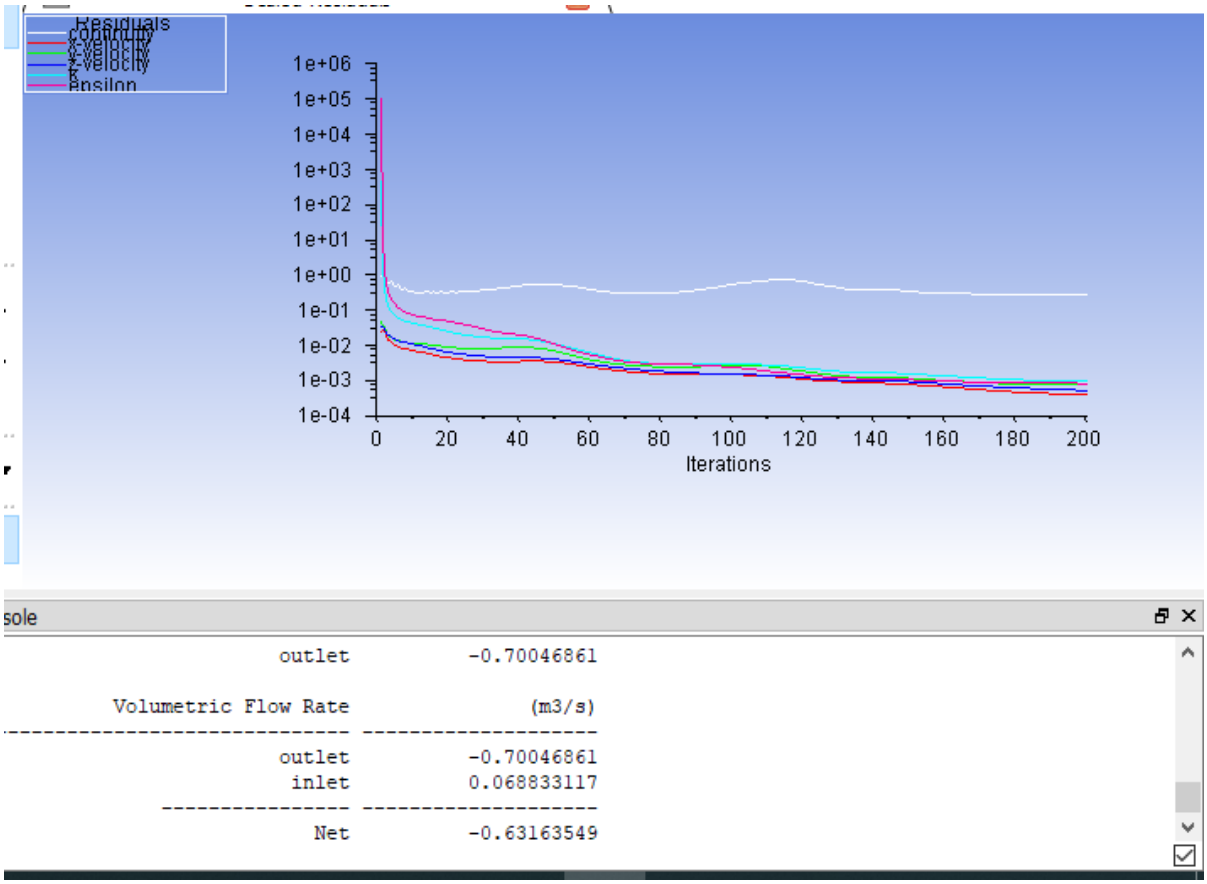

Volume Flow rate

4.5.Optimization:

After the validation of the bladeless fan model, the next step involved optimizing its design to achieve a higher flow rate. The optimization process aimed to enhance the performance of the fan by modifying key parameters such as the height of the airfoil, slit thickness, outlet angle, and diameter of the circular geometry.

To begin the optimization, variations of the bladeless fan design were created by systematically changing the before mentioned parameters. For each design iteration, the analysis was performed using the simulation model to evaluate its performance and assess the resulting flow characteristics. The various parameters that were changed are as shown:

No. of Designs	Length(mm)	Height(mm)	Outlet angle	Outlet Separation (mm)
1	100	20	16	1.3
2	100	25	16	1.3
3	100	30	10	1.3
4	100	30	13	1.3
5	100	30	16	1.3
6	100	30	16	1
7	130	40	10	1.3
8	130	40	10	1

The analysis involved simulating the airflow within the fan for each design variation and determining the resulting flow rate. The flow rate represents the amount of air passing through the fan per unit of time and is a crucial performance metric for evaluating the effectiveness of the design.

The optimization process continued by assessing each design iteration and comparing its flow rate with the desired performance objectives. The objective was to identify a design that yielded a satisfactory flow rate improvement while considering other factors such as feasibility and practicality.

After multiple iterations and evaluations, a specific bladeless fan design was identified as the most satisfactory. This optimized design no.6 featured a height of the airfoil measuring 30cm, a slit thickness of 1mm, an outlet angle of 16 degrees, and a circular geometry with a diameter of 30cm. The flow rates of all design analyzed for optimization are shown.

Design Nu	Volumetric Flow rate (CFM)
1	1594
2	1467
3	1490
4	1542
5	1482
6	1637
7	1529
8	1423

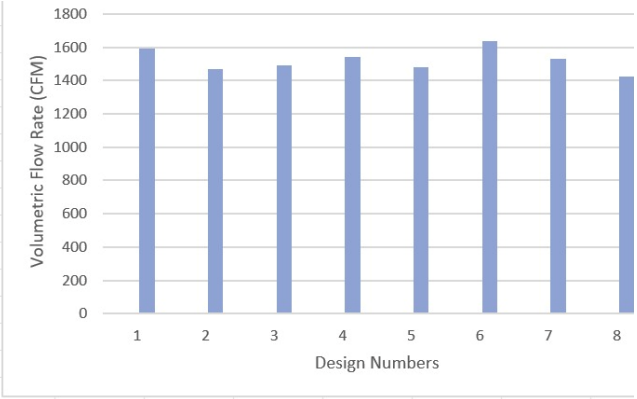

The result of this optimized design was a significantly increased flow rate. Specifically, the output flow rate of the bladeless fan was approximately 13 times higher than the inlet flow rate. This improvement indicated the successful achievement of the desired objective to enhance the fan's performance and increase the amount of airflow it generated.

By conducting a systematic optimization process and analyzing the performance of different design variations, the bladeless fan design with the specified dimensions was identified as the most favorable solution. This optimized design demonstrated a notable improvement in flow rate, indicating its potential for enhanced efficiency and effectiveness in practical applications.

Overall, the optimization phase ensured that the bladeless fan design was refined to maximize its performance and meet the desired objectives. The optimized design, with its specific parameters, provided a significant increase in flow rate and represented an improved solution compared to the initial design.

4.6.Results of the Finalized Model:

Using the Ansys software, the volume flow rate of the airflow through the bladeless fan was calculated. This parameter provides an indication of the amount of air passing through the fan.

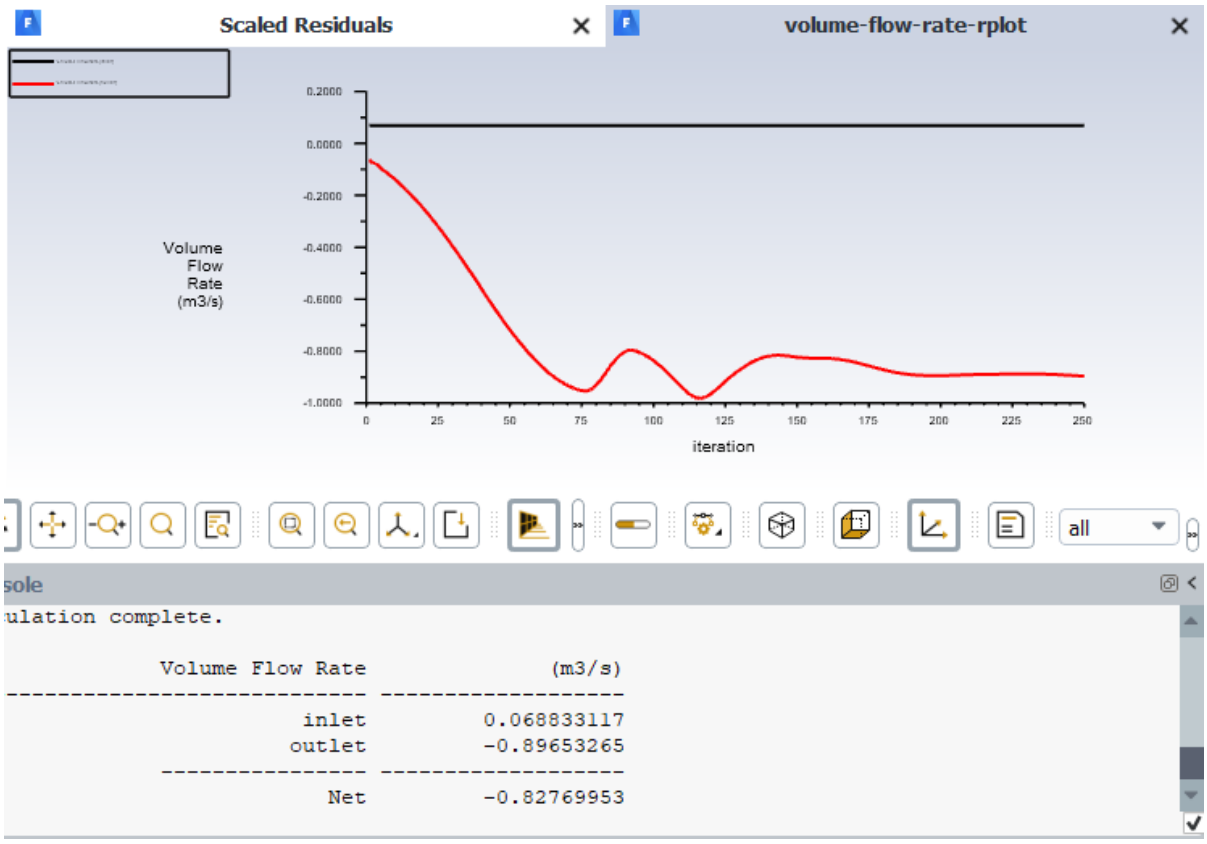

Volume flow rate

Additionally, the velocity and pressure contours were visualized to understand the distribution and variations of these parameters across the bladeless fan. The velocity contour shows the magnitude and direction of the airflow at different points within the fan, while the pressure contour illustrates the distribution of air pressure.

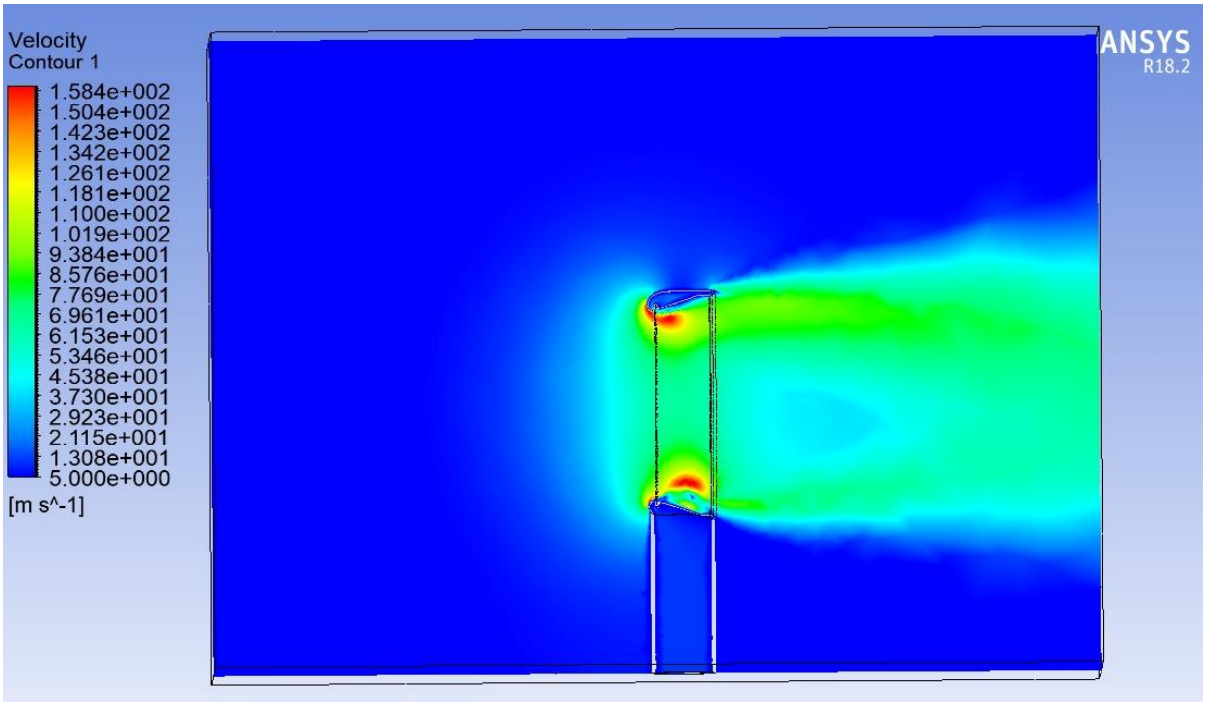

Velocity Contour

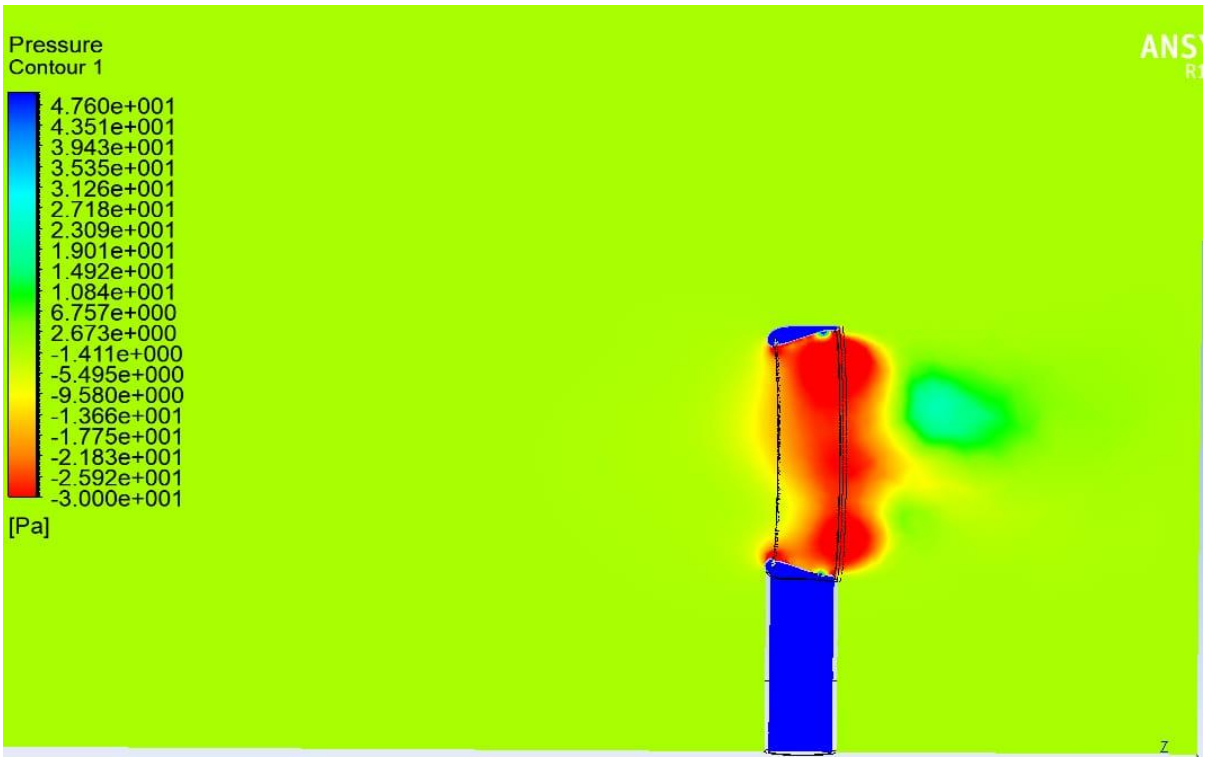

Pressure Contour

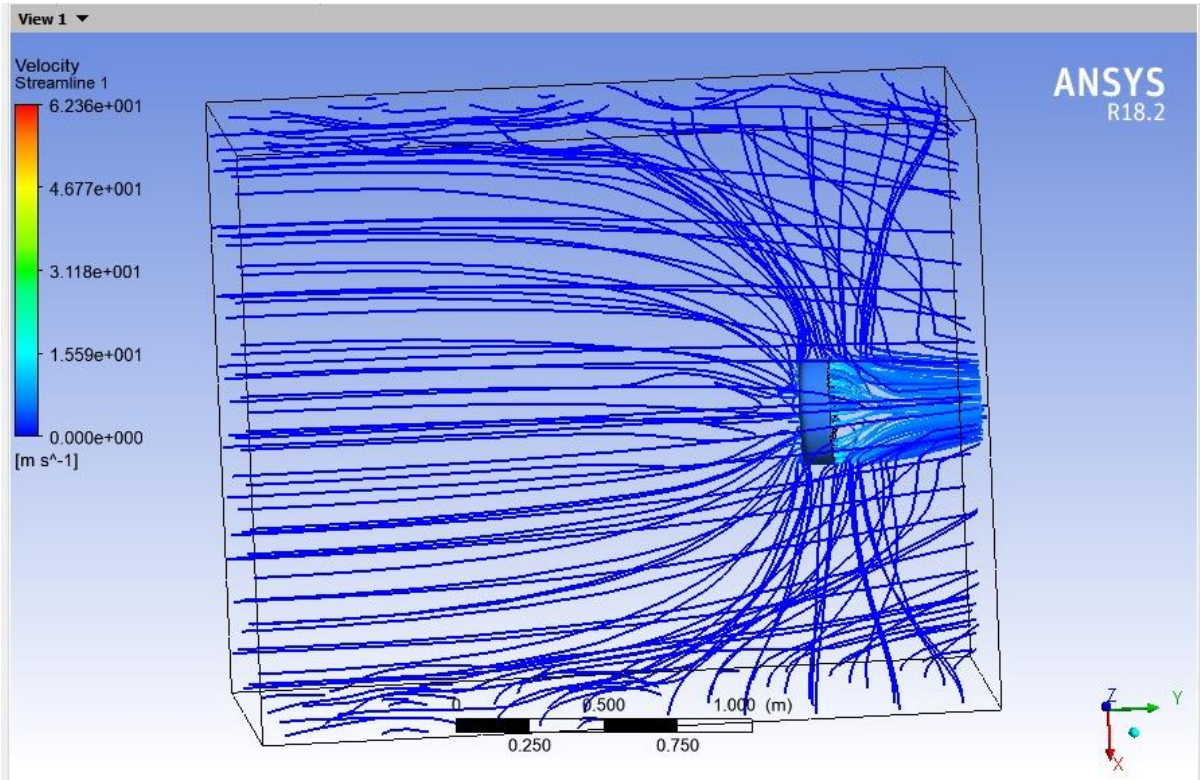

Velocity Streamline

Furthermore, the streamlines, which represent the paths traced by imaginary particles in the airflow, were observed to comprehend the flow patterns generated by the bladeless fan. These streamlines provide valuable insights into how the air moves and interacts with the fan structure.

5. 3D Modeling & Structural Analysis

5.1.Design of ring:

The ring of the bladeless fan was meticulously crafted using computer-aided design (CAD), taking into careful consideration the results obtained from computational fluid dynamics (CFD) analysis and the inherent limitations of the fabrication process. This particular ring was meticulously designed to possess a hydraulic diameter of precisely 26 centimeters, which, after thorough investigation, was determined to be the maximum viable dimension for

the 3D printing procedure employed. Therefore, to ensure optimal performance and adherence to manufacturing constraints, the ring was meticulously fashioned with an exact hydraulic diameter of 26 centimeters, coupled with a slender yet sturdy slit thickness of 3 millimeters.

In the pursuit of engineering excellence, the design of the ring drew inspiration from the renowned Eppler 473 ring model. The meticulousness extended to aligning the ring's profile in precise accordance with the insights gleaned from the CFD analysis. Every contour and curve were thoughtfully crafted to ensure seamless integration with the intended airflow patterns, facilitating optimal aerodynamic efficiency.

Behold the masterpiece that emerged from this intricate design process—a stunning CAD model of the ring that brings together the amalgamation of scientific inquiry, practical considerations, and aesthetic finesse. This meticulously developed CAD representation showcases the intricacies and minute details that went into the creation of this essential component of the bladeless fan, serving as a testament to the tireless efforts undertaken to optimize its performance and manufacturing feasibility.

The dedication to precision and attention to detail in crafting the ring of the bladeless fan on CAD, guided by the findings from CFD analysis and mindful of the constraints inherent in the fabrication process, have culminated in a remarkable achievement. The resultant CAD model stands as a testament to the pursuit of engineering excellence, embodying a harmonious blend of scientific knowledge and innovative design.

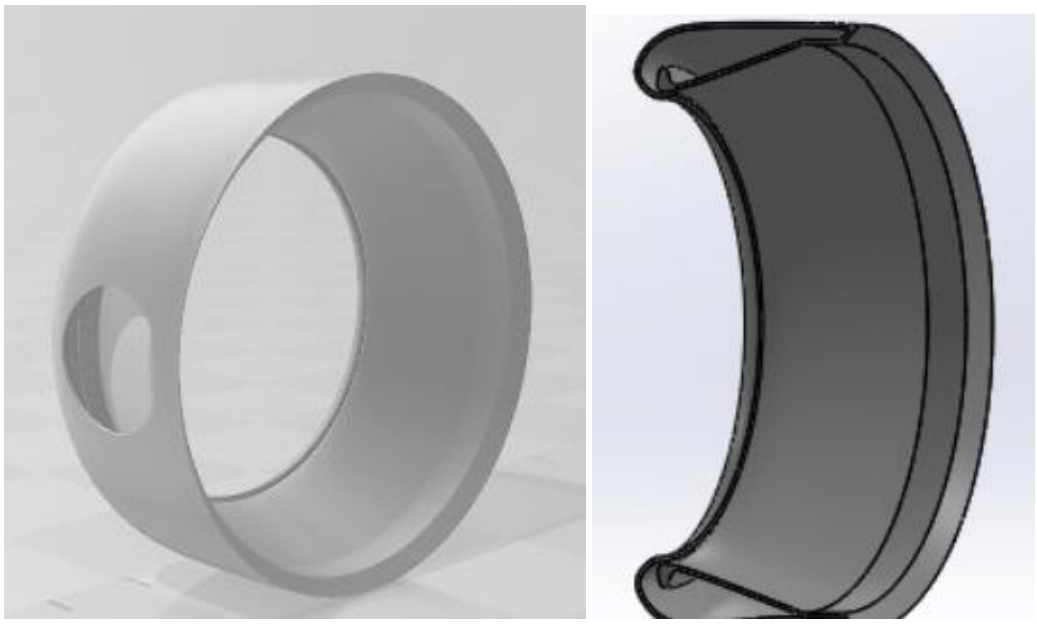

5.2.Modelling of impeller housing:

The impeller housing plays a pivotal role within the bladeless fan, as it serves as the crucial component where the motor is securely mounted. Additionally, it encompasses strategically placed apertures that facilitate the intake of external air, subsequently propelling it outwards through the ring. Ensuring the robustness and impeccable design of this housing is of utmost importance to counteract potential deformations arising from motor vibrations. Moreover, the design must strike a balance between strength and cost-effectiveness during the manufacturing process.

To seamlessly integrate with the ring, the impeller housing was meticulously crafted with a diameter of 8 cm, allowing for a seamless fit within the ring's aperture. The housing was thoughtfully structured to incorporate secure mounts that accommodate the motor, providing a stable foundation for optimal performance. The circumferential arrangement of four lines of triangular holes in the housing enables efficient airflow management, ensuring a consistent and powerful output. As depicted in the accompanying figure, the base of the housing was positioned at a height of 13 cm, where it gracefully transitions into a curve, ultimately reaching a maximum height of 14 cm at the pinnacle. This intentional design choice not only

enhances the visual appeal but also contributes to the housing's structural integrity and longevity.

To strike a harmonious balance between functionality and affordability, the width of the impeller housing was purposefully set at 1.5 cm. This dimension ensures the necessary strength and durability while optimizing the cost of production, thus making the fan accessible to a wider range of consumers. Additionally, two strategically placed apertures were incorporated into the housing design to facilitate seamless connectivity to the power supply and the inclusion of a potentiometer, enabling precise control over the volume flow rate.

The CAD model provided below visually encapsulates the meticulous attention to detail and thoughtful engineering that went into crafting the impeller housing, resulting in a product that seamlessly combines functionality, durability, and cost-efficiency.

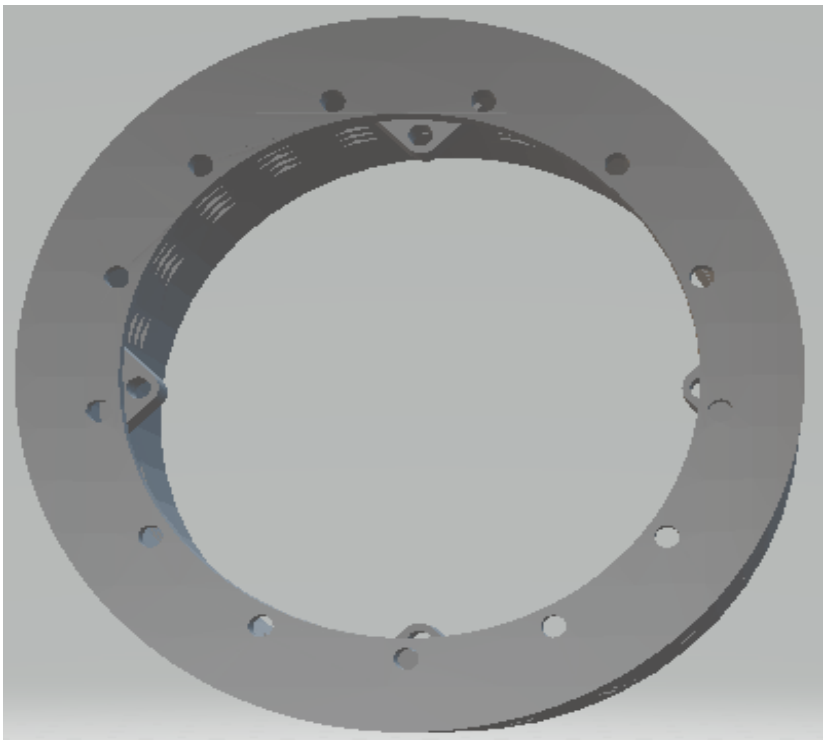

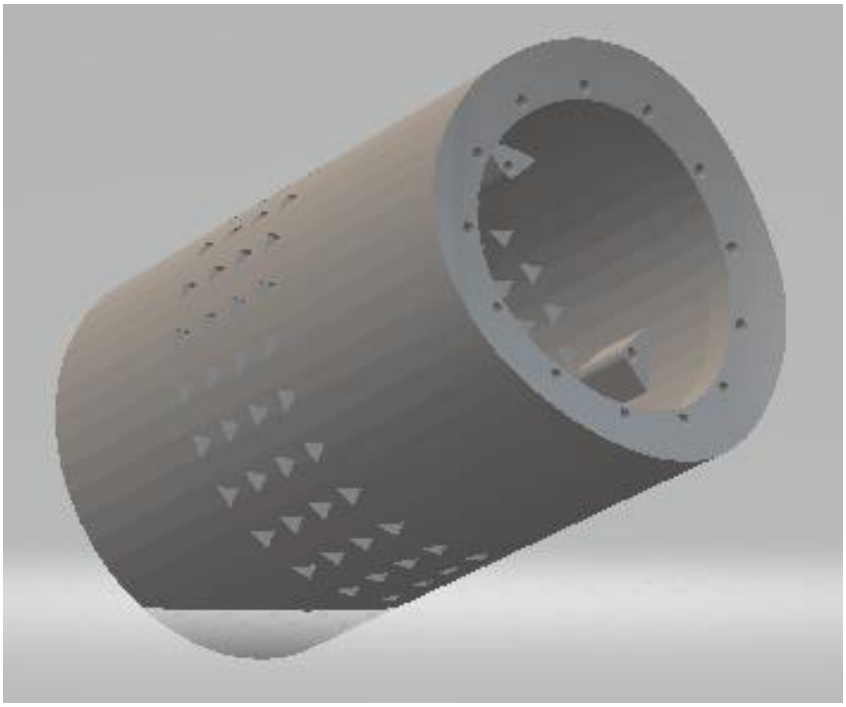

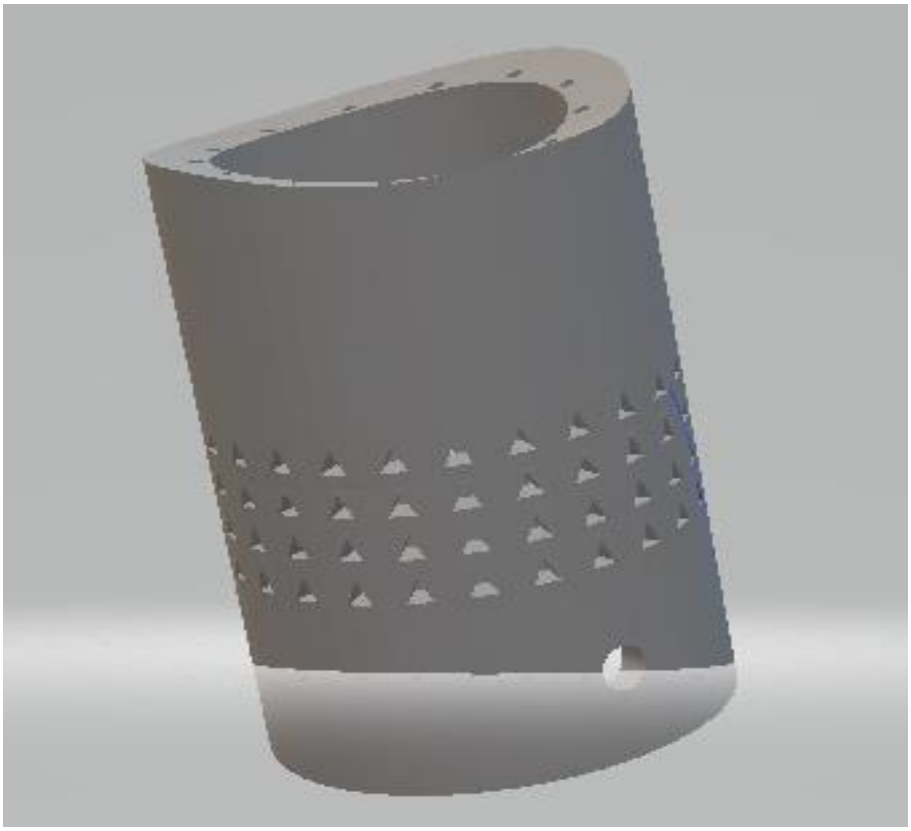

5.3.Stand for impeller housing:

We have accomplished a remarkable breakthrough in the realm of bladeless fan design, revolutionizing the way we experience cooling comfort. Our innovative approach involves the integration of a meticulously crafted stand for the impeller housing, which serves a dual purpose beyond mere mounting. Notably, this ingenious stand concept boasts an exceptional feature: the provision of additional space that enables a more substantial intake of ambient air.

In the pursuit of enhancing the fan's performance, we conscientiously set the height of the stand at an optimal 1 centimeter. This specific measurement has been carefully determined to strike the perfect balance, providing the ideal amount of clearance necessary to facilitate the unhindered flow of incoming air. By introducing this measured elevation, we ensure an expansive air inlet, thereby enabling a more efficient and effective suction process.

The profound impact of this design modification is exemplified by the amplified volume of air drawn inward. As a direct consequence of the enlarged air inlet facilitated by our purpose-built stand, an increased quantity of ambient air is seamlessly channeled through the fan's mechanisms. This amplified influx of air, rich in cooling potential, culminates in an enhanced airflow at the outlet.

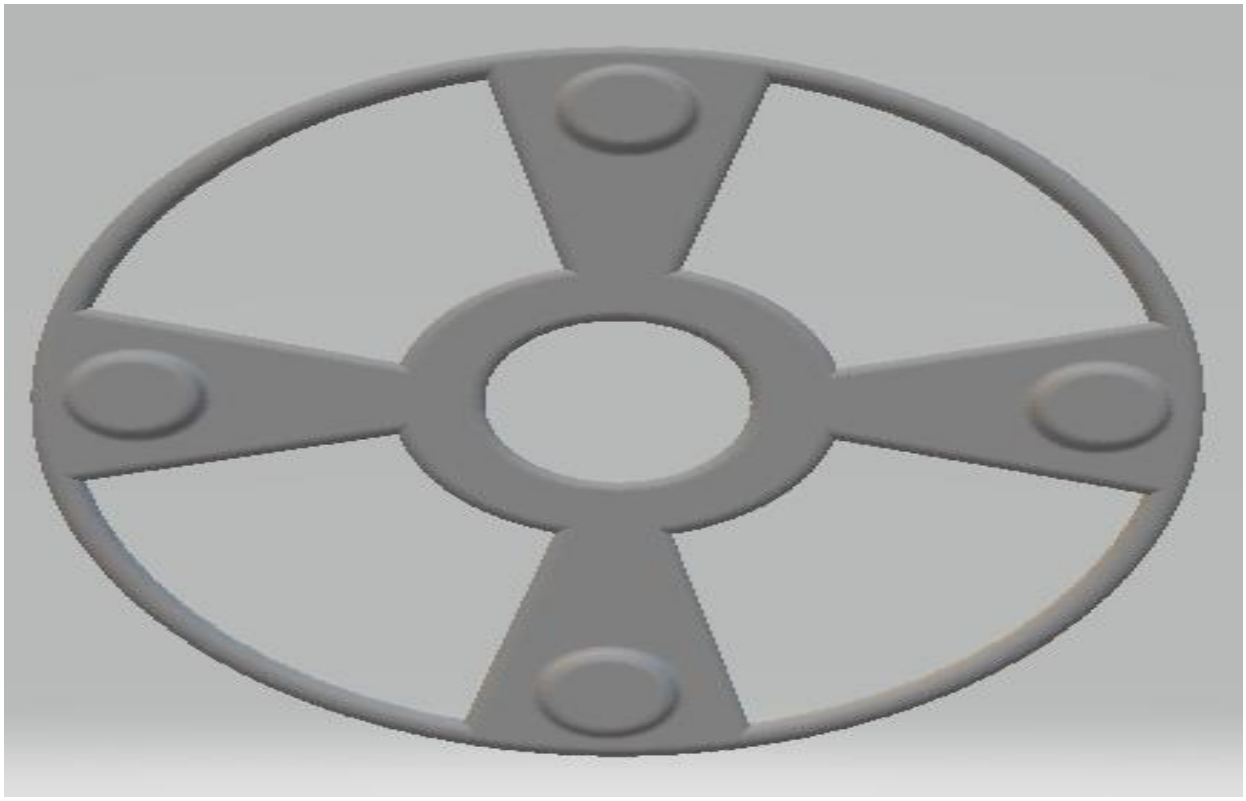

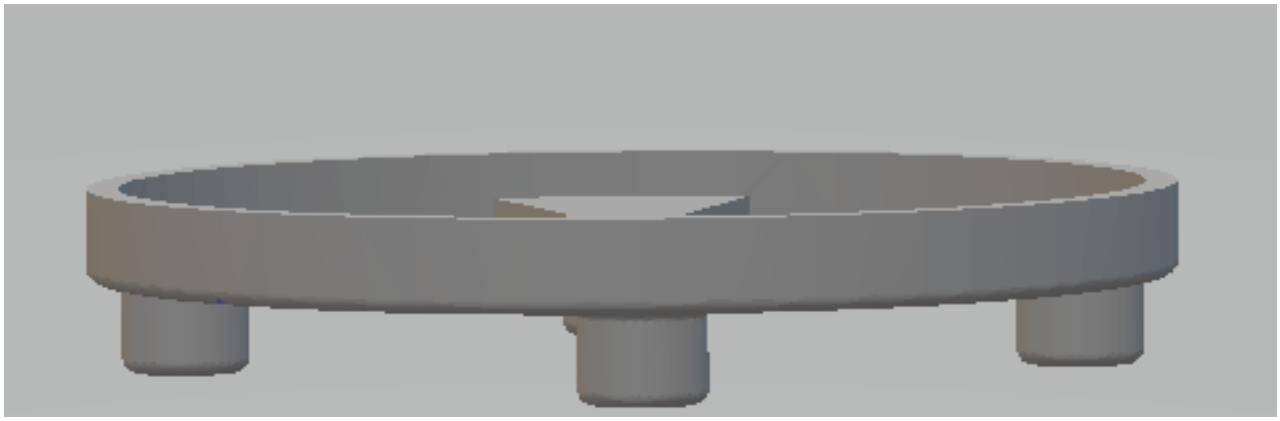

5.4.Assembly and rendering of design:

The process of bringing together the three aforementioned components is accomplished through the utilization of CAD modelling techniques. This intricate and meticulous process

involves the assembly of the various parts, culminating in the creation of a comprehensive and visually compelling representation of the fan.

The assembly phase, carried out within the realm of CAD, serves as a pivotal step in manifesting the overall appearance of the fan. Through a careful arrangement of the components, each meticulously positioned to ensure optimal functionality and aesthetic appeal, a comprehensive depiction of the fan emerges.

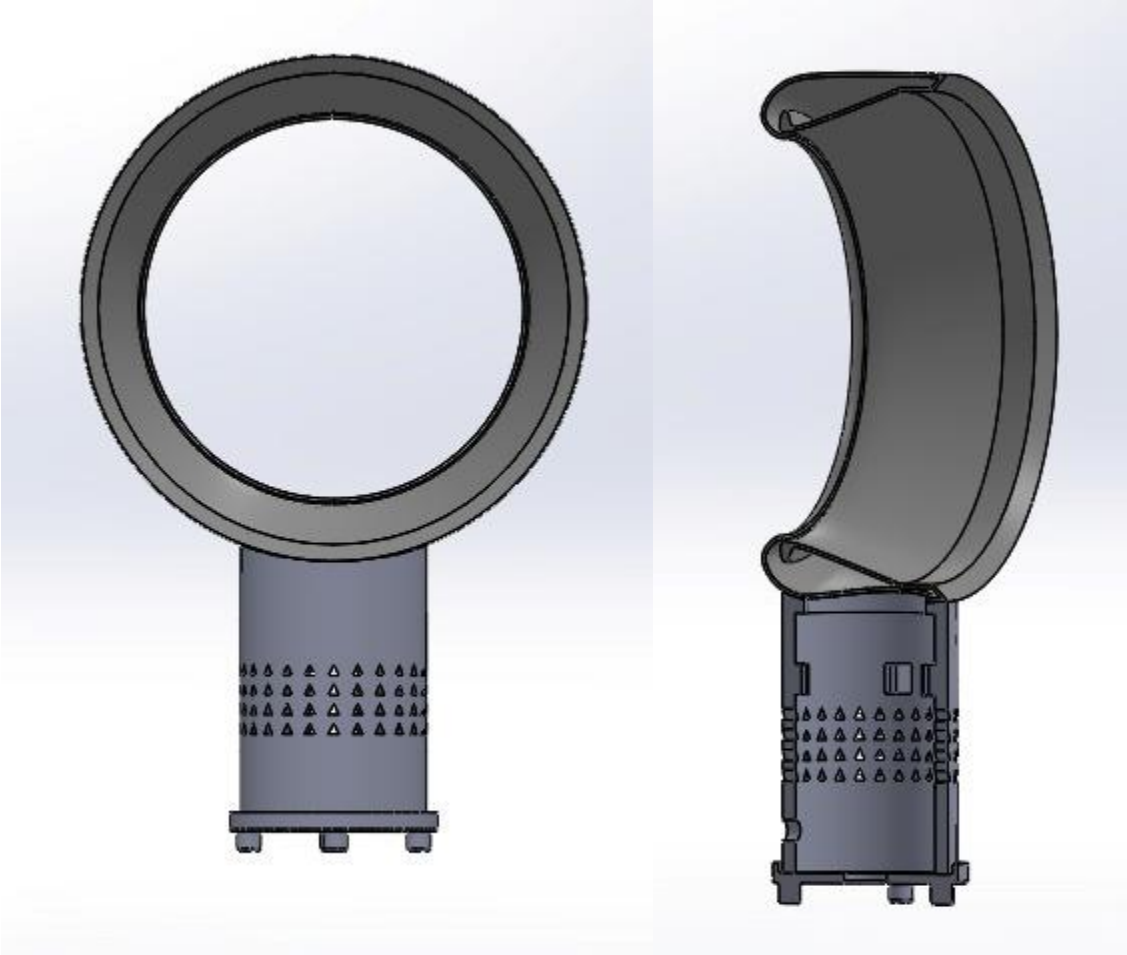

To further enhance the visual aspects of the fan assembly, the implementation of advanced software such as Blender comes into play. This sophisticated tool is employed to render the assembled fan, imbuing it with an additional layer of captivating aesthetics. By utilizing the powerful capabilities of Blender, the fan assembly is transformed into a lifelike and visually striking representation, showcasing its intricate details, sleek contours, and overall design finesse.

5.5.Static Structural Analysis:

The strength evaluation of the model was conducted through a meticulous static structural analysis using ANSYS Workbench. The primary objective was to accurately determine the robustness of the impeller housing, as it serves as a critical component responsible for enduring significant loads. Consequently, the focus of the analysis was directed towards the examination of the housing's performance under the weighty motor load.

To simulate real-world conditions, a load of precisely 50 grams was individually applied in the negative y-axis direction on each mounting point of the impeller housing. A fixed support was thoughtfully implemented beneath the base of the structure to provide stability during the analysis. A load of 350 grams equal to the weight of the upper ring is applied at the connection point on the upper curve of the housing. The ensuing results, which are presented in the accompanying figure, offer a comprehensive visual representation of the implications of the applied load on the structure.

Upon careful examination of the figure, it becomes evident that certain areas of the impeller housing exhibit discernible deformations. Although these deformations are relatively minor in magnitude, they are localized within a specific region. This observation is of utmost importance as it enables a comprehensive understanding of the housing's behavior under the imposed load and facilitates an evaluation of its overall safety.

By employing ANSYS Workbench for static structural analysis, we have gained valuable insights into the deformations experienced by the impeller housing under the weight load of the motor. The in-depth examination of these results allows us to make informed decisions regarding necessary design modifications or reinforcement measures to enhance the structural integrity and ensure the long-term reliability of the housing.

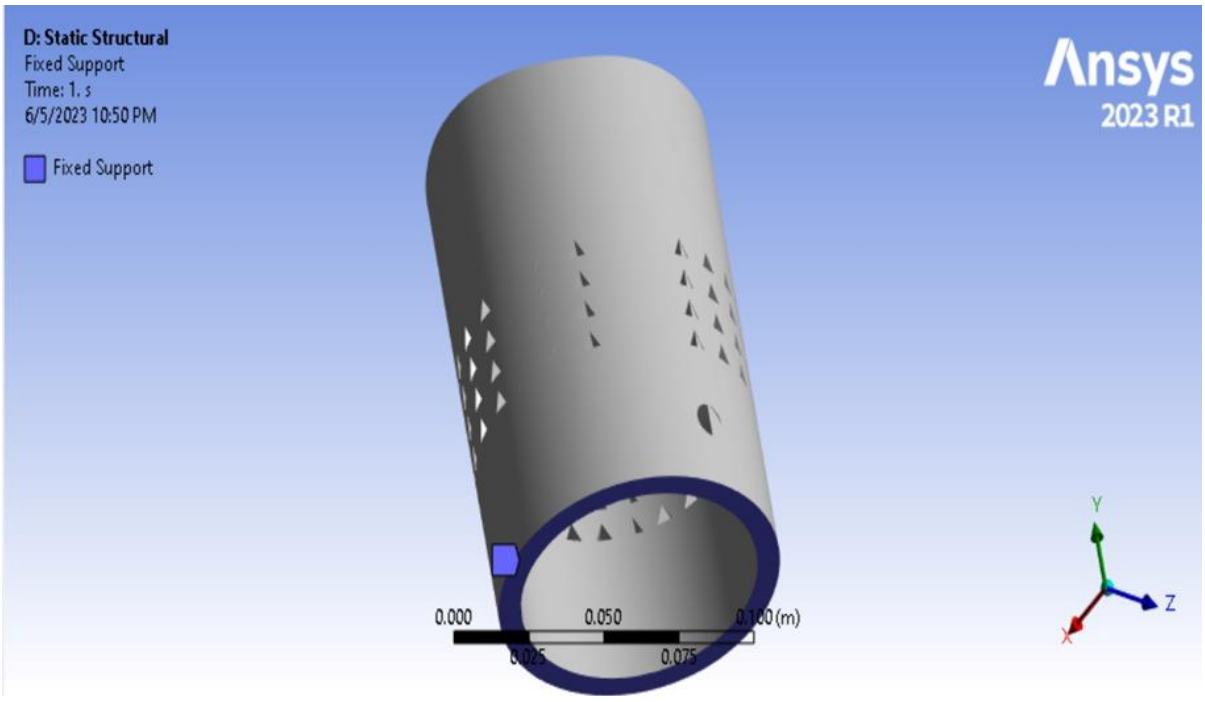

Fixed Support

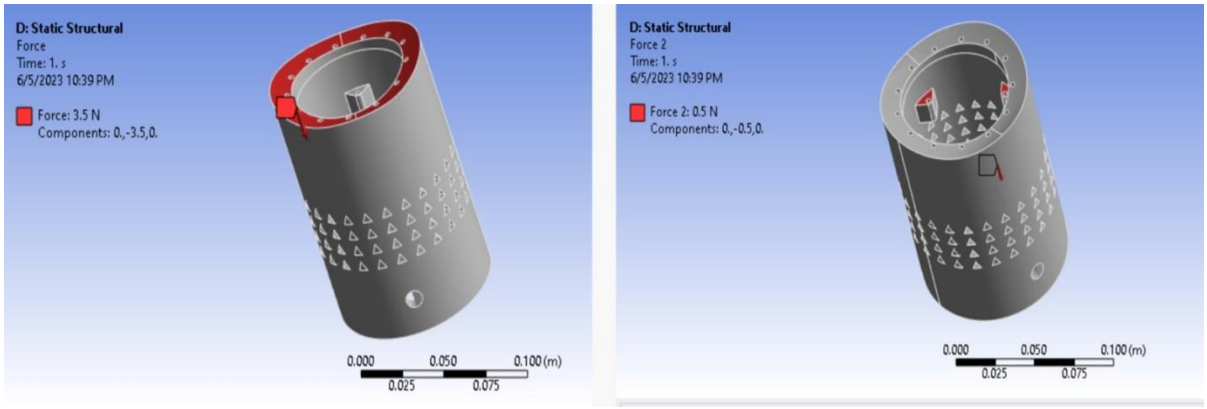

Forces

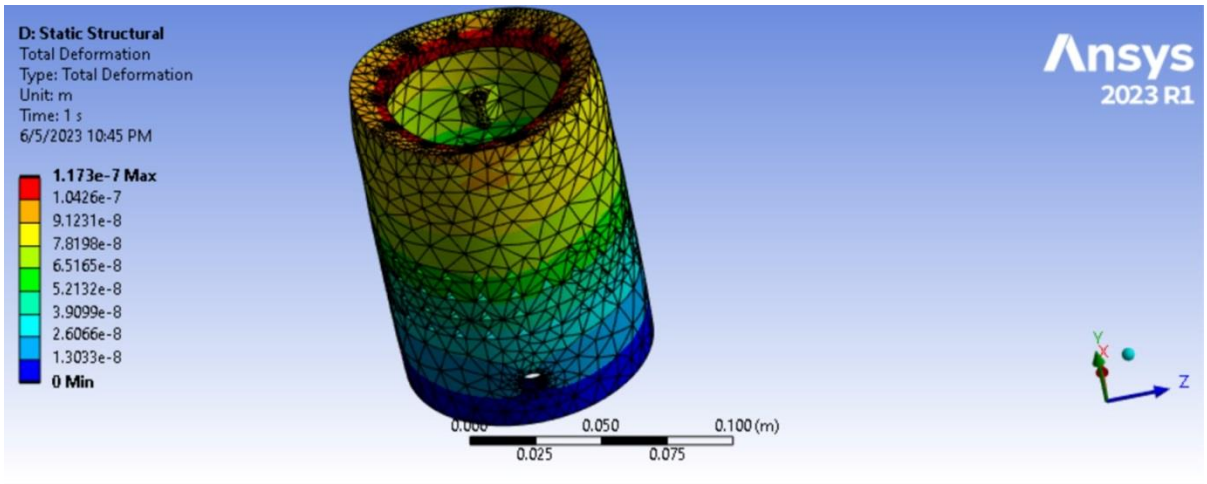

Deformation

5.6.Modal Analysis:

The fundamental objective of conducting a modal analysis is to identify and determine the natural frequencies at which the modes of vibrations are likely to manifest within a given system. These vibrations possess the potential to induce consequential deformations or even result in the failure of specific components or parts. Consequently, the outcomes derived

from a comprehensive modal analysis are crucial in shedding light on the frequencies at which these modes are anticipated to occur. For the specific case at hand, an extensive examination has been undertaken, encompassing a meticulous analysis of ten distinct modes of vibration.

	Frequency [Hz]	Amplitude [m]	Phase Angle [°]
1	22.04	8.9131e-010	179.94
2	26.08	8.9131e-010	179.93
3	30.12	8.9131e-010	179.92
4	34.16	8.9131e-010	179.91
5	38.2	8.9131e-010	179.9
6	42.24	8.9131e-010	179.89
7	46.28	8.9131e-010	179.88
8	50.32	8.9131e-010	179.87
9	54.36	8.9131e-010	179.86
10	58.4	8.9131e-010	179.85
11	62.44	8.9131e-010	179.84
12	66.48	8.9131e-010	179.83
13	70.52	8.9131e-010	179.82
14	74.56	8.9131e-010	179.81
15	78.6	8.9131e-010	179.8
16	82.64	8.9131e-010	179.79
17	86.68	8.9131e-010	179.78
18	90.72	8.913e-010	179.77
19	94.76	8.913e-010	179.76
20	98.8	8.913e-010	179.75
21	102.84	8.913e-010	179.74
22	106.88	8.913e-010	179.73
23	110.92	8.913e-010	179.72
24	114.96	8.913e-010	179.7
25	119.	8.913e-010	179.69

These are the frequencies at which the modes will occur. While the motor we chose is of 14500 rpm or 221.46 Hz. So, our structure is safe under the dynamic load of the motor.

6. Fabrication

Bladeless fan will be fabricated using 3D printer. Following are some points regarding to fabrication:

6.1.Reasons for choosing 3d printing:

- Cost-effective: 3D printing allows for the creation of a prototype model at a fraction of the cost of traditional manufacturing methods. This can save money on materials and labor costs.
- Speed: 3D printing can create a prototype model in a matter of hours or days, compared to weeks or months with traditional manufacturing methods. This allows for faster product development and testing.
- Customization: 3D printing allows for the creation of unique and customized designs, such as the bladeless fan prototype. This can lead to more innovative and efficient products.
- Flexibility: 3D printing allows for the creation of prototypes in various materials, such as plastics and metals. This allows for more realistic testing and evaluation of the prototype model.
- Environmentally friendly: 3D printing reduces the need for large-scale production and the use of harmful chemicals, leading to a more sustainable manufacturing process.
- Design Improvements: 3D printing makes it easier to make design changes, so it's easy to make improvements and modifications to the prototype model. This allows for a more efficient product development process.

6.2.Material Used for 3D Printing:

- PLA+ is a modified version of PLA (polylactic acid) that offers improved strength and durability compared to standard PLA.
- PLA+ is less brittle than standard PLA, making it more suitable for functional prototypes that need to withstand some level of stress or movement.
- PLA+ can be printed at lower temperatures, which can reduce warping and improve the overall quality of the print.
- PLA+ can be used with a wider range of nozzle sizes and extruder temperatures, providing more flexibility in the printing process.
- PLA+ is also biodegradable and made from renewable resources, making it more environmentally friendly than some other 3D printing materials.

- PLA+ is a good choice for bladeless fan prototypes because it is strong enough to withstand the forces generated by the fan and is less brittle than standard PLA, reducing the chances of the prototype breaking during testing.

6.3.Components:

Our revolutionary bladeless fan incorporates a cutting-edge brushless DC motor, accompanied by an intelligently designed asymmetrical fan consisting of five meticulously crafted blades. The motor itself boasts an impressive power rating of 27W, ensuring optimal performance and efficiency. One of the standout advantages of our bladeless fan lies in its unparalleled ability to generate an output flow rate while consuming power that is a staggering 60% lower compared to conventional table fans.

To regulate the air flow rate with utmost precision and convenience, we have integrated a potentiometer into our design. This ingenious device seamlessly interfaces with a sophisticated Wheatstone bridge circuit, intelligently incorporated into the fan's printed circuit board (PCB). This impeccable arrangement allows for effortless control over the air flow rate, empowering users to customize their cooling experience to their exact preferences.

When it comes to power supply, our bladeless fan offers unparalleled versatility. By incorporating a DC jack, we have ensured compatibility with a wide range of power sources. Whether utilizing a standard AC supply or opting for an alternative source, our fan seamlessly converts the input to a stable DC supply, guaranteeing reliable and efficient operation. The DC jack serves as the vital link between the power supply and the potentiometer, facilitating seamless communication and coordination between the various components.

In essence, the circuitry within our bladeless fan culminates in a comprehensive and sophisticated mechanism for controlling the air flow rate. With every element working harmoniously in unison, users can revel in the superior cooling capabilities of our fan, all while effortlessly adjusting the airflow to suit their individual comfort levels.

6.4. 3D printed parts and assembly:

Displayed below are the three remarkable components crafted through the ingenious process of 3D printing: the exquisite ring, the meticulously designed impeller housing, and the sturdy stand. Notably, the impeller housing boasts an integrated circuit that seamlessly melds with its structure, exemplifying a harmonious fusion of functionality and aesthetics.

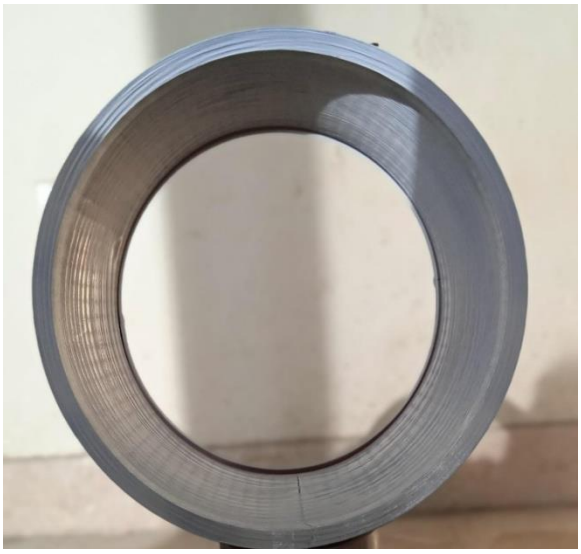

Ring

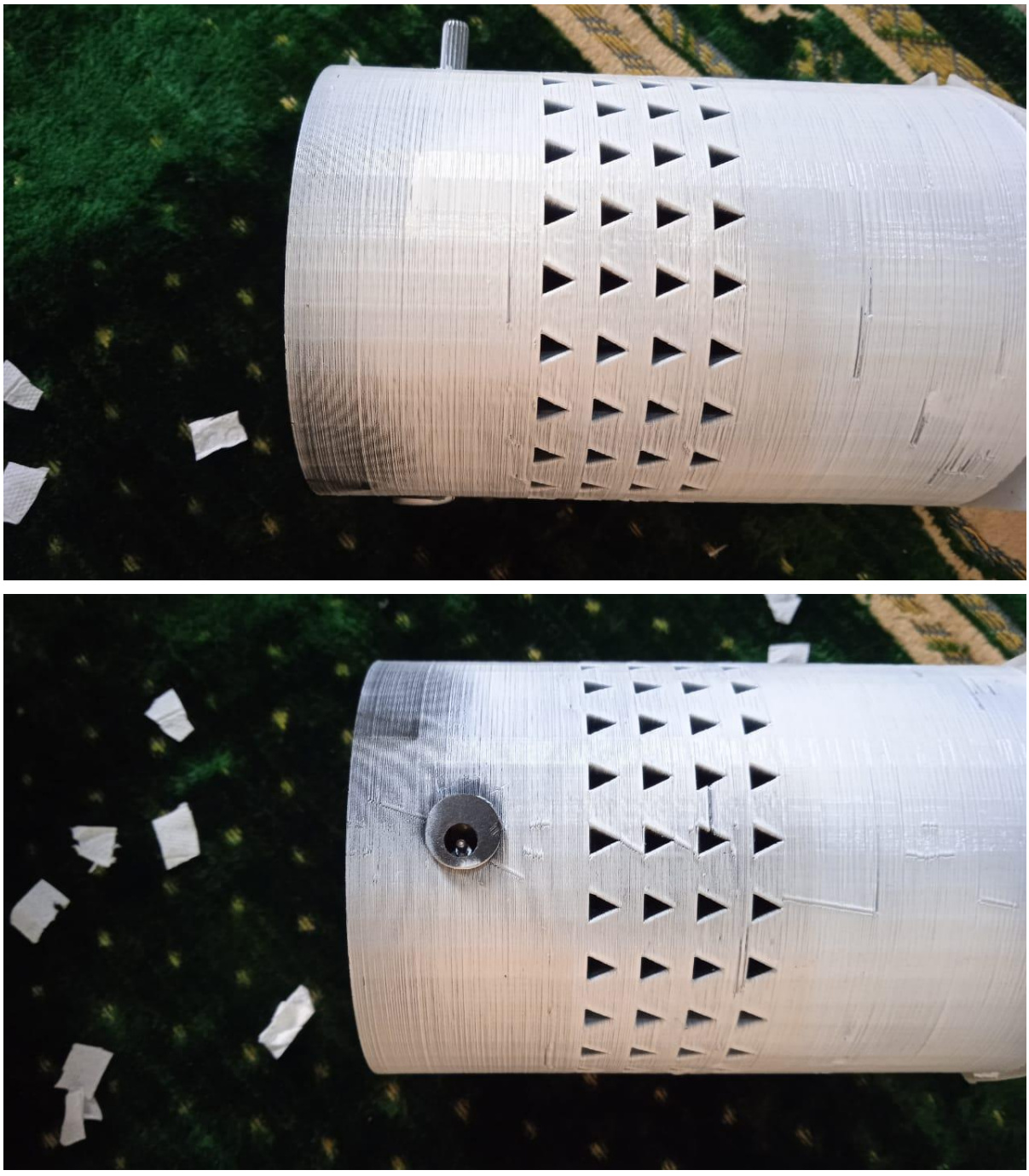

Impeller Housing

Stand

To ensure a flawlessly unified assembly, a formidable adhesive known as depoxi was employed, effortlessly forging an unyielding bond between the three aforementioned 3D printed parts. This judicious choice of adhesive serves a dual purpose, guaranteeing a robust connection while simultaneously fortifying the assembly against the infiltration of undesirable air leakage from any susceptible crevices or seams.

By adopting this astute approach, the creators of this masterpiece have effectively eliminated any potential weaknesses that could compromise the structural integrity of the assembly. The employment of depoxi not only exemplifies their unwavering commitment to precision engineering but also serves as a testament to their unwavering pursuit of perfection in crafting a flawless, hermetically sealed product.

Final Assembly

7. References

- http://researchgate.net/
- https://www.sciencedirect.com/science/article/pii/S111001681500191X
- https://atomberg.com/blog/post/bladeless-fan
- https://businesspartnermagazine.com/top-features-youll-need-high-end-bladeless-fan/
- https://docs.lib.purdue.edu/herrick/232/
- Design Study of a Bladeless Fan “Air Multiplier” Manish Daiya Lecturer, Mechanical Department, KJIT, Vadodara, Gujarat
- https://www.yourbestdigs.com/